



Lawrence Berkeley Laboratory

UNIVERSITY OF CALIFORNIA

Materials & Molecular Research Division

Submitted to Surface Science

THE DECOMPOSITION OF AMMONIA ON THE FLAT (111)
AND STEPPED (557) PLATINUM CRYSTAL SURFACES

W.L. Guthrie, J.D. Sokol, and G.A. Somorjai

February 1980

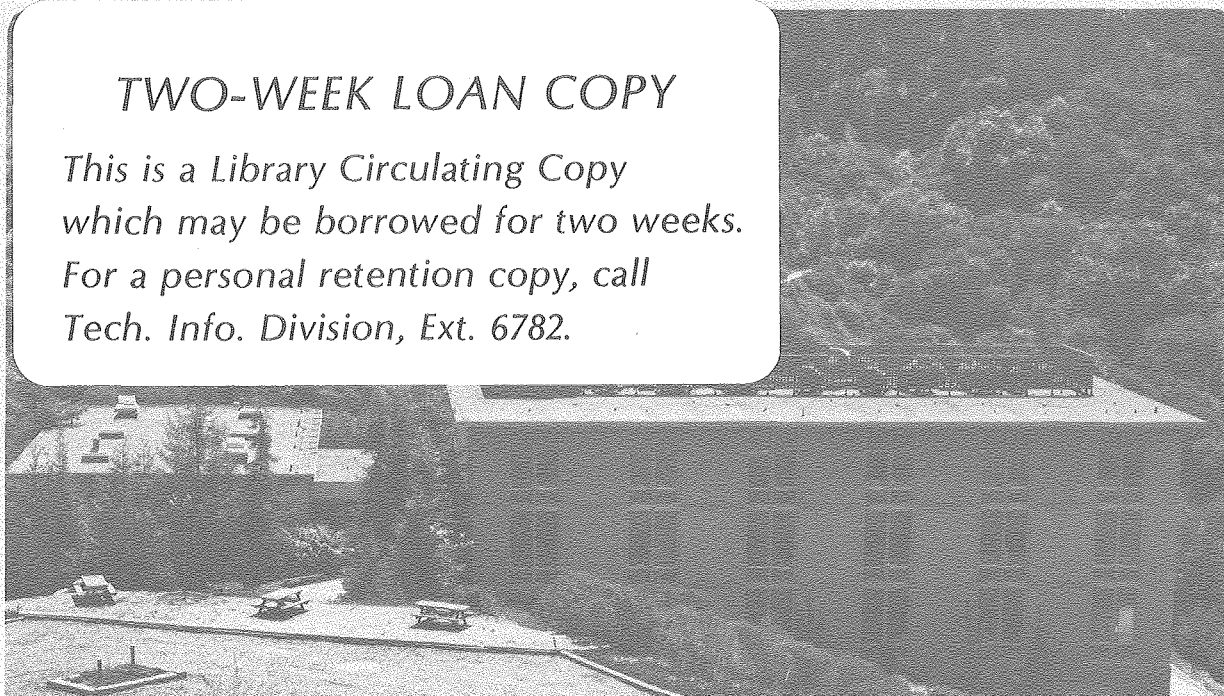
RECEIVED
LAWRENCE
BERKELEY LABORATORY

FEB 9 1981

LIBRARY AND
CURRENTS SECTION

TWO-WEEK LOAN COPY

*This is a Library Circulating Copy
which may be borrowed for two weeks.
For a personal retention copy, call
Tech. Info. Division, Ext. 6782.*



LBL-10536 c.2

DISCLAIMER

This document was prepared as an account of work sponsored by the United States Government. While this document is believed to contain correct information, neither the United States Government nor any agency thereof, nor the Regents of the University of California, nor any of their employees, makes any warranty, express or implied, or assumes any legal responsibility for the accuracy, completeness, or usefulness of any information, apparatus, product, or process disclosed, or represents that its use would not infringe privately owned rights. Reference herein to any specific commercial product, process, or service by its trade name, trademark, manufacturer, or otherwise, does not necessarily constitute or imply its endorsement, recommendation, or favoring by the United States Government or any agency thereof, or the Regents of the University of California. The views and opinions of authors expressed herein do not necessarily state or reflect those of the United States Government or any agency thereof or the Regents of the University of California.

THE DECOMPOSITION OF AMMONIA ON THE FLAT (111) AND STEPPED (557)
PLATINUM CRYSTAL SURFACES

W.L. Guthrie, J.D. Sokol^{*} and G.A. Somorjai

Materials and Molecular Research Division, Lawrence Berkeley
Laboratory, and Department of Chemistry, University of
California, Berkeley, CA 94720

Abstract

Ammonia adsorption, desorption and decomposition to H_2 and N_2 has been studied on the flat (111) and stepped (557) single crystal faces of platinum using molecular beam surface scattering techniques. Both surfaces show significant adsorption with sticking coefficients on the order of unity. The stepped (557) surface is 16 times more reactive for decomposition of ammonia to N_2 and H_2 than the flat (111) surface. Kinetic parameters have been determined for the ammonia desorption process from the Pt(111) surface. The mechanism of ammonia decomposition on the (557) face of platinum has been investigated.

*Permanent Address: Microwave Associates, Inc., Burlington, MA 01830

This manuscript was printed from originals provided by the authors.

Introduction

The formation and decomposition of ammonia has been studied extensively on supported and unsupported metal catalysts. Interest in catalytic reactions of ammonia stem from an incomplete understanding of the mechanisms of its catalyzed synthesis, which include the dissociation of dinitrogen and the formation of N-H bonds as elementary steps.¹ Studies of the ammonia decomposition probe the properties of the N-H bonds of ammonia. We have investigated the kinetics and mechanism of ammonia decomposition on the flat Pt(111) and the stepped Pt(557) single crystal surfaces. Using molecular beam relaxation spectroscopy (MBRS),^{2,3} the experiments were conducted in an ultrahigh vacuum system which incorporated the surface analytical techniques of low energy electron diffraction (LEED) and Auger electron spectroscopy (AES). These techniques determine, respectively the surface structure and surface composition. Use of single crystal samples permitted exploration of the structure sensitivity of the N-H bond breaking. The pulsed molecular beam surface scattering technique provided information about the sticking probability and reaction probability of the incident molecule upon a single collision with the surface as well as information on the residence time of adsorbed species. The use of isotope exchange (NH_3+D_2) permitted exploration of the onset of N-H bond breaking as the reaction conditions (crystal and reactant temperature, surface structure, reactant pressure) were varied. As a result, a physical picture of the kinetics and mechanism of ammonia decomposition was obtained.

Experimental

The experiments reported here were performed using an ultrahigh vacuum molecular beam surface scattering apparatus, shown schematically in Figure 1. This apparatus has been described elsewhere⁴ so only details pertinent to the current ammonia decomposition studies will be discussed here.

The beam was formed in the source chamber by flow of the source gas (3-60 Torr) through a 0.01" orifice under nearly effusive conditions. For most of the experiments reported, the source gas was anhydrous ammonia (Matheson, 99.99%) used without further purification; however, for the ammonia-deuterium exchange experiments, a mixture of anhydrous ammonia and D₂ (99.7%) was used. The molecular beam was chopped in the differential chamber by a slotted disc chopper with a range of chopping frequencies of 5 to 150 cps. The beam was passed into the UHV scattering chamber where it impinged upon the sample surface. The single crystal samples were heated radiatively. The crystal temperature was measured by a chromel-alumel thermocouple spot welded to the edge of the sample. The scattered reactants and reaction products were detected by a quadrupole mass filter which is rotatable in the scattering chamber about the crystal surface. The filtered ion current was detected by a channeltron multiplier and processed using a lock-in amplifier to measure the component of the mass spectrometer signal at the incident beam chopping frequency.

The scattered beam and product molecule signals were measured using the differential or integral modes described previously.⁵ In the differential mode the mass spectrometer is positioned to measure the flux of molecules emitted at a particular scattering angle. In the integral mode the mass spectrometer is positioned out of line-of-sight of the crystal surface, and

the modulation in partial pressure of the species emitted from the surface is measured. The integral mode signal is proportional to the total rate at which the molecules are emitted from the surface, i.e. it is proportional to the differential mode signal integrated over all angles of emission.

The amplitude and phase lag of the integral mode signal vary as a function of chopping frequency because the emitted molecules have a finite residence time in the UHV chamber before being pumped away. To first approximation it can be shown that the amplitude, r , and phase lag, ϕ , behave according to Equations 1a and 1b,

$$r \propto \frac{g}{(\omega^2 + (s/v)^2)^{1/2}} \quad (1a)$$

$$\tan \phi = \frac{v\omega}{s} \quad (1b)$$

where g is the rate of emission from the surface, ω is the chopping frequency, s is the effective pumping speed, and v is the UHV chamber volume.

The effective pumping speed depends on the gas, so the attenuation and phase lag will vary for the different species detected. Therefore, it is necessary to determine for each species the attenuation and phase lag resulting from the finite residence time in the UHV chamber so that these effects can be removed from the reactive scattering data. The effects of the chamber residence time can be determined by scattering the gas of interest from a surface at high temperatures to assure negligibly short surface resident time, and measuring the attenuation and phase lag as a function of incident beam chopping frequency. In this circumstance, Figure 2 shows this measurement for nitrogen. The solid line corresponds to the values predicted by Eq.1, showing that the scattering behavior is more complex than that predicted by the simple model.

In reporting the integral mode data, the scattered beam and product molecule signal phase lags have been corrected by subtracting the phase lags produced by the molecule's finite residence time in the UHV chamber, so that the reported phase lags are the result of crystal surface residence times. Attenuation resulting from chamber residence time was not corrected for in reporting the product molecule signal amplitude, but was accounted for in the reaction model calculations.

For differential mode measurements, the product signals were normalized with respect to the incident beam intensity monitored by positioning the mass spectrometer in the beam flux. For integral mode measurements, product signals were normalized with respect to the ammonia integral mode signal from scattering from the very hot (~ 1300 K) surface.

Two single crystal surfaces of platinum were studied, Pt(111) and Pt(557). Their atomic structure is shown schematically in Figure 3. The samples were mechanically polished and etched in dilute aqua regia. Sample orientations were verified by the use of back reflection X-ray Laue diffraction and were within 1° of the desired orientation. Prior to each experiment, surfaces were cleaned in situ by a combination of argon ion bombardment and chemical cleaning. The surfaces received two 20 minute argon ion treatments at ion energies of 900 eV and 600 eV and a sample temperature of 1050 K. Argon ion bombardment was followed by 20 minutes of chemical cleaning in oxygen at a background oxygen pressure of 2×10^{-7} Torr, and a sample temperature of 800 K. After flashing and annealing in vacuum at a sample temperature of 1200 K, the surface was free of contaminants and well ordered as determined by Auger electron spectroscopy (AES) and LEED. In the course of the experiments, the samples were flashed to 1200 K after each data point

was taken. The frequent flashing prohibited the slow poisoning of the decomposition reaction and made the data reproducible.

Results

A. NH_3 scattering from the Pt(111) crystal face.

The data obtained for ammonia scattering from the Pt(111) crystal face are shown in Figures 4a, 4b, 4c, and 4d. The incident ammonia beam was formed with a source backing pressure of 15 Torr, and the integral mode was used for detection. The chopping frequencies are 5 cps, 20 cps, 50 cps, and 150 cps. The amplitude and phase of the scattered ammonia signal at the chopping frequency are plotted along with the expected response from the most successful model (see Discussion) to describe the scattering mechanism.

It is helpful to introduce the sticking coefficient, s , which we define as the fraction of the incident molecules which are adsorbed into states with detectable residence times. The 'nonsticking' molecules could adsorb into a state with a residence time which is finite yet too short to be detected (<0.2 ms). Inspection of Figure 2b reveals the salient features of ammonia scattering from Pt(111). At low temperatures the ammonia residence time is long compared to the modulation period and the molecules desorb at random times with respect to the chopped beam. These dephased molecules contribute to the zero frequency (d.c.) component of the scattered ammonia signal and are not detectable at the fundamental frequency. Thus only the molecules which do not stick contribute to the amplitude at low temperatures. At high temperatures the residence time of the molecules is shorter than the modulation period, and all of the ammonia desorbs in phase.

The transition from the low temperature to the high temperature behavior occurs at temperatures where the residence time becomes comparable to the modulation period. In the transition region, there is a sudden increase and decrease in the phase lag as a function of crystal temperature along with the change in ammonia signal amplitude. The temperature of the transition increases as the chopping frequency increases.

A fraction of the incident ammonia molecules decomposes on a single scattering from the surface. The hydrogen product molecule phase and amplitude data from ammonia decomposition on the Pt(111) surface are shown in Figure 5. The H_2 signal was collected in the integral mode and is shown normalized to the 1250 K ammonia signal. No correction was made for the differences in detection efficiencies for the two gases. However, the maximum H_2 signal corresponds to about 1% ammonia decomposition as determined by comparison of the data shown in Figure 5 to the amount of decomposition observed on the Pt(557) surface. The signals are small and the background noise large, which leads to the scattering in the graph. Due to the difficulties of the measurements, the data monitored at the lowest chopping frequency, 5 cps, is the most reliable and the only one shown.

The rate for H_2 production from NH_3 decomposition increases, then decreases with temperature, reaching a maximum at approximately 750 K. The H_2 phase lag at 5 cps is large for temperatures less than 750 K, indicating that the H_2 production from NH_3 is slow at the lower temperatures. From this limited data the kinetics of ammonia decomposition on the Pt(111) surface appears to be similar to that on the (557) surface. The major difference is the fraction of incident ammonia decomposed; the (557) surface

is approximately 16 times more reactive for decomposition (see below).

The angular distribution of the scattered ammonia was measured at 1250 K and was found to be nearly cosinelike about the surface normal (Figure 6a). A cosine scattering distribution is usually assumed to infer adsorption and thermal accommodation, although recent measurements have shown that this is not always the case.⁶ The angular distribution observed could imply that a significant fraction of incident ammonia is still adsorbing and desorbing at the higher temperatures and is thermally accommodated on the surface.

Residence times for adsorbed ammonia molecules are long at 375 K, on the order of 0.1 second. If an angular distribution is measured with a chopping frequency of 100 cps, the sticking molecules will be largely dephased and effectively masked from the observed distribution. It is then possible to observe the scattering of the 'nonsticking' molecules (those with mean residence times less than 0.2 ms). Such an angular distribution is shown in Figure 6b. The scattering distribution has a large component which peaks near the specular angle (50°) as well as a diffuse background. There are two potential contributions to the diffuse background. The sticking molecules will make a small contribution to the amplitude at 100 cps. The second source is large angle scattering of the nonsticking molecules. The specular behavior exhibited by a significant fraction of the nonsticking molecules would imply elastic or inelastic scattering without adsorption.

The dependence of the sticking coefficient, as determined by the low temperature amplitude of the scattered ammonia signal, on beam intensity, is shown in Figure 7. The sticking coefficient decreases with increasing beam intensity. This could result from a coverage dependence in the sticking

coefficient which has been observed in other systems.⁷ The variation in the sticking coefficient over experimentally accessible beam pressures is small. The sticking coefficient is apparently still rising at the lowest pressure, which implies that we can only measure a lower bound to the zero coverage sticking coefficient.

The sticking coefficient was constant for changes of beam temperature from 300 to 500 K, and was only weakly dependent on the angle of incidence of the beam.

Figure 8 shows the differential mode signal amplitude for product ND_3 ($m/e=20$) from a scattered mixed beam of NH_3 and D_2 . The beam angle of incidence was 45° , the detector was placed at the surface normal. The beam source backing pressure used was 55 Torr. The ratio of D_2 to NH_3 partial pressures in the source was 4.5/1.0. The excess D_2 was required to be able to carry out the reaction independent of the deuterium surface concentration. However, practical values of the ratio were limited by the need for enough NH_3 to detect the products and by the pumping speed of the source chamber. For this experiment the product amplitude signal is normalized with respect to the amplitude of the ammonia signal in the direct beam. The amplitude of the product ND_3 signal reaches a maximum at 600 to 650 K, and declines for higher and lower temperatures. The ND_3 product signals were too small to allow reliable phase lag measurements. If the exchange reaction on the Pt(111) surface is similar to that on the stepped Pt(557) surface, then the decline in the amplitude of the ND_3 signal at lower temperatures is at least partly due to signal dephasing caused by the long surface residence time of the molecules. (see below)

B. NH_3 scattering from the Pt(557) crystal face

The data obtained for ammonia scattering from the stepped Pt(557)

crystal face are shown in Figure 9. The magnitude of the scattered ammonia signal along with the ammonia signal phase lag are plotted as a function of crystal temperature in Figures 9a, 9b, and 9c for incident beam chopping frequencies of 5 cps, 20 cps, and 50 cps, respectively. The behavior of the scattered ammonia is qualitatively similar to that on the Pt(111) surface (Figure 4). There is significant adsorption as indicated by the sharp phase lag maximum and the decline in scattered signal amplitude at lower temperatures.

There are minor differences in the scattered ammonia signal for the two surfaces. The maximum phase lag is significantly smaller for the stepped Pt(557) surface and the signal amplitude at lower temperatures is slightly larger. There is a gradual dip in the amplitude of the scattered ammonia signal for temperatures between 600 K and 900 K. This fall in amplitude is due to decomposition on the surface as can be seen from the H₂ and N₂ product signals in Figure 10a. Figure 10b shows the corrected H₂ and N₂ phase lags as a function of crystal temperature for a 5 cps chopping frequency. Other nitrogen containing products were searched for, but none were found.

The major difference between the (111) and (557) surfaces of Pt is the increase reactivity of the stepped (557) surface for ammonia decomposition. Here the H₂ product signal is roughly 16 times larger than that from the flat (111) surface (Figure 5). At 700 K, where the H₂ product signal is at its maximum, approximately 18% of the incident ammonia decomposes, as can be seen by the corresponding dip in the scattered ammonia amplitude (Figure 9).

The H₂ and N₂ phase lags are large for temperatures less than 700 K (Figure 10b), suggesting slow rates in the pathways for H₂ and N₂

production. It is clear that the N_2 phase lags are significantly larger than the H_2 phase lags. The mean time for the decomposition products to appear in the gas phase is much greater for N_2 than for H_2 . The large phase lags account for the steep rise in the H_2 and N_2 signal amplitude near 700 K. The phase lags demodulate the signal and decrease the detected amplitude. The zero frequency H_2 product amplitude would increase much more gradually and should mirror the fall in amplitude of the scattered ammonia signal. The H_2 signal amplitude and phase lag as a function of crystal temperature for 20 cps and 50 cps chopping frequencies are shown in the appendix with the reaction model mechanism behavior (Figure A3). The data is not corrected for the differences in sensitivity for H_2 and NH_3 or for the frequency dependent attenuation of the integral mode signal resulting from the scattered molecules' finite residence time in the UHV chamber.

The dependence of the H_2 and N_2 phase lags on the beam intensity at 725 K is shown in Figure 11. The N_2 phase lag shows a detectable rise at decreasing beam intensities, whereas the H_2 phase lag is essentially constant. This indicates the nature of the rate limiting steps in the respective NH_3 decomposition reaction pathways, as is discussed below.

Figure 12 shows the dependence of the amplitude of scattered NH_3 , H_2 , and N_2 on incident ammonia beam intensity (or incident flux). For the purpose of determining apparent reaction order, the scattered amplitudes and incident beam intensity are plotted logarithmically. The scattered ammonia amplitude at 1250 K was used to measure beam intensity because of the saturation of the Channeltron multiplier at the high ion flux encountered in direct beam measurements. The reaction orders in ammonia determined from the slopes are 0.87 for H_2 , and 0.98 for N_2 . Scattered ammonia has a slope of 1.05. Within error, these values are unity.

To determine the effect of angle of incidence on the decomposition reaction the incident angle was varied by rotating the crystal manipulator and the H_2 signal amplitude was recorded at 725 K. No change was observed in the amount of H_2 produced with changing angle of incidence. The crystal was mounted such that the beam was normal to the step edges.

The decomposition showed no dependence on beam temperature. To measure the beam temperature dependence, the ^{beam source} oven temperature was raised to 475 K, and the measurements of Figures 9 and 10 were repeated. There was no detectable change in the ammonia or H_2 signals for all crystal temperatures.

To observe the isotope exchange on the stepped Pt(557) surface, a mixed beam of NH_3 and D_2 was produced. The gases were mixed by adjusting the gas flows through two leak valves in the source manifold. The ratio of D_2 and NH_3 partial pressures in the source was 2.7/1.0. The beam angle of incidence was 45° , and the scattered products were detected in the differential mode at the angle of the surface normal. All possible isotope species were observed with qualitatively similar temperature dependencies (Figure 13). In this experiment there is additional exchange in the source and on the walls of the chamber. The background signals have been subtracted from the data, but contribute to the scatter in the data. The NH_2D signal ($m/e=18$) has been corrected by subtracting the expected signal from cracking of the ND_3 and NHD_2 products in the ionizer. The small amplitude of the differential mode exchange product signal and the subtraction of the background signals caused large errors in the exchange product phase lag data. The phase lag errors are inversely proportional to the signal amplitude and so are smallest from 550 K to 750 K. In this temperature range the ND_3 ($m/e=20$) phase lag is zero. Above 750 K the error in phase lag increases dramatically, but the phase lag appears to remain constant near zero.

Below 550 K the error in phase lag again increases, and it appears that the phase lag increases steadily with lower temperatures to about 400 K, which is the lowest temperature at which data was taken for the exchange reaction. Therefore, the low temperature falloff in exchange product signal amplitude is due to dephasing of the signals. The true exchange probability (zero frequency limit of the signal amplitude) would not fall as rapidly and may continue to increase.

It is interesting to compare the temperature dependence of the exchange reaction to the temperature dependence of the decomposition reaction (Figure 14). Here the results of two experiments are plotted in the same figure--the ammonia and hydrogen signal amplitudes from the decomposition experiments (Figures 9 and 10), and the ND_3 amplitude from the exchange experiment. These signal amplitudes are affected by signal dephasing. The figure shows that the exchange reaction has essentially ceased where the for maximum NH_3 decomposition is reached. The temperature range temperature range/of the exchange reaction overlaps the lower portion of the temperature range for the decomposition reaction (500-700 K).

To investigate isotope effects for the incident ammonia, a beam of ND_3 (Merck, Sharpe, and Dohme, 99%) was formed with a source backing pressure of 5 / ^{Torr} and scattered from the Pt(557) surface. The incident beam was chopped at 20 cps, and the amplitude and phase/^{lag} of scattered ND_3 and product D_2 were measured. The behavior of ND_3 on the (557) surface of Pt is very similar to the behavior of NH_3 . The normalized scattered signal amplitude at 20 Hz reaches ~ 0.25 for ND_3 , compared to $.40$ for NH_3 at 375 K. The respective maximum phase lags at low temperatures are ~ 14 and ~ 24 for NH_3 and ND_3 . This indicates a slightly larger adsorption probability for ND_3 than for NH_3 , which may be due to easier conversion of translational to vibrational energy via the more closely spaced vibrational levels in ND_3 .

At all temperatures measured, the phase lag for the product D_2 signal is essentially equal to the H_2 phase lag from NH_3 scattering. The product D_2 signal amplitude appears to be a few percent larger than the H_2 signal amplitude indicating a slightly higher probability for decomposition per incident molecule for ND_3 than for NH_3 , which is most probably due to the larger sticking coefficient for ND_3 .

Discussion

A. Ammonia adsorption-desorption kinetics on Pt(111)

The methods for analysis of modulated molecular beam reaction scattering data and the behavior of a number of linear and nonlinear reactive surface processes have been discussed in detail.^{2,3,8-11} We have used least squares fitting of surface reaction models to analyze the Pt(111) ammonia scattering data.¹² In this circumstance the decomposition channel is neglected since about 1% of the incident ammonia decomposes. Several surface reactions models were proposed, then the parameters for each model were adjusted to give the best least squares agreement to the data. The simplest model which gave good agreement with the observed scattering data was chosen. Our data for ammonia scattering from Pt(111) was adequately fit by a model with temperature independent adsorption followed by a desorption process with one rate-limiting step.

The ammonia signal (Figure 4) shows adsorption behavior with a long residence time at low temperature. From the magnitude of the phase lag at a chopping frequency of 5 cps, we can estimate that the mean residence time is of the order of 0.1 seconds at 375 K. The sticking molecules are dephased, leaving the nonsticking molecules as the only contribution

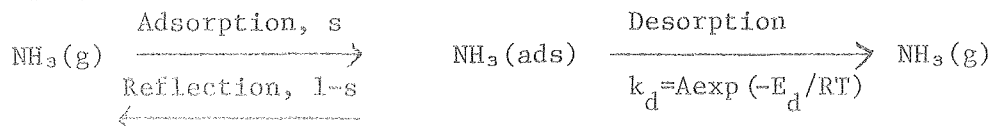
to the low temperature asymptotic value of the scattered NH_3 amplitude. The low temperature value of the signal amplitude should approach the value $1-s$ so that the sticking coefficient is $s=0.75$.

The ammonia phase lag behavior can be explained in terms of the separation of the scattered molecules into two fractions. The fraction $1-s$ of molecules which are nonsticking, and the fraction s which stick. Each fraction contributes to the scattered ammonia signal with its own amplitude and phase. The nonsticking molecules contribute a temperature independent component to the normalized scattered ammonia signal. This component has an amplitude of $1-s$ and zero phase lag. The fraction of molecules that stick contributes a component of amplitude s and zero phase lag at high temperature. With decreasing temperature the phase lag of this component increases and the amplitude decreases. The total normalized scattered ammonia signal is a vector sum of the two components; the net effect is that the phase lag passes through maximum and then approaches zero with decreasing temperature.

Changes in beam temperature in the range of 300--500 K have no effect on the sticking coefficient. It appears that the adsorption probability is nearly independent of the incident beam angle of incidence and the incident beam intensity.

Measurement of the angular distribution of the scattered ammonia gives an indirect indication of adsorption. The scattered ammonia distribution at 1250 K is diffuse, which is an indication that at that temperature there is adsorption-desorption behavior for a significant fraction of the incident molecules. This analysis of the ammonia scattering from the Pt(111) surface leads to the simple model that was constructed and is

shown here.



This model gave the best agreement to the data. It consists of an associative adsorption followed by a desorption process with one rate limiting step. The probability of adsorption, s , was assumed to be coverage and temperature independent. The desorption process could be one first-order step or a number of series steps leading to desorption as long as one of the steps is rate limiting.

Using the notation of Olander, et al.,³ the normalized integral mode scattered ammonia signal, I_{NH_3}/I_0 , corresponding to the reaction model above is

$$I_{\text{NH}_3}/I_0 = (1-s) \frac{sk_d}{(i\omega + k_d)} \quad (2)$$

for incident beam flux, I_0 , chopping frequency, ω , sticking coefficient, s , and desorption rate k_d . The amplitude, r , and phase lag, ϕ , behavior are given by

$$r_{\text{NH}_3} = (1-s) \sqrt{1 + \frac{s(2-s)k_d^2}{\omega^2 + k_d^2}} \quad (3a)$$

and

$$\tan \phi_{\text{NH}_3} = \frac{\omega s k_d}{\omega^2 + k_d^2 - \omega^2 s} \quad (3b)$$

For this adsorption-desorption model, it is possible to extract approximate values for the kinetic parameters from the data. As previously noted, s can be determined from the low temperature behavior of the scattered ammonia amplitude, $r_{\text{NH}_3} \xrightarrow{\text{low } T} 1-s$ at low temperature.

The temperature for which the phase lag is a maximum, $T_{\phi_{\text{max}}}(\omega)$ satisfies the relation between k_d , ω , and s

$$k_d(T_{\phi_{\text{max}}}(\omega)) = s\sqrt{1-s} \quad (4)$$

and the maximum value of the phase lag is

$$\tan \phi_{\text{max}} = \frac{s}{2\sqrt{1-s}} \quad (5)$$

Further, the desorption energy E_d determines the temperature width of the phase lag data around the maximum phase lag. By expanding the tangent of the phase lag as a Taylor series about the maximum, the width in temperature of the maximum can be shown to be approximately

$$\Delta T_{\text{FWHM}} \sim \frac{2 RT^2 \phi_{\text{max}}}{E_d} \quad (6)$$

The kinetic parameter resulting from the least squares minimization for the reaction model are

$$\begin{aligned} s &= 0.73 \\ 10^{10} A &= 10.4 \pm 0.9 \text{ sec}^{-1} \\ E_d &= 15.4 \pm 0.4 \text{ kcal/mole.} \end{aligned}$$

The curves representing the expected response of the reaction model are plotted with the data in Figures 4a, 4b, and 4c. Within the limits of the errors in the data and the assumptions made in the model, the agreement between the calculated and measured scattering behavior is good. The agreement lends some justification to the assumption made in the reaction model that the sticking coefficient is nearly independent of coverage or beam and crystal temperature for the coverages examined, and that the decomposition does not greatly affect the adsorption-desorption processes.

The sticking coefficient measured here agrees fairly well with other experiments for ammonia on platinum which give values of s near unity.¹³ As noted above, the value is a lower limit to the zero coverage sticking coefficient.

The ammonia desorption energy was measured by Gland¹³ on a stepped platinum surface with large terrace width. Due to the widths of the terraces, this surface could be expected to behave similarly to a Pt(111) surface. The desorption energy measured by thermal desorption was 18.4

kcal/mole, which is larger than the 15.4 kcal/mole measured here. However, Gland assumed a pre-exponential factor of 10^{13} sec^{-1} in calculating the desorption energy. Insertion of the pre-exponential measured here into Gland's data yields a lower desorption energy of $E_d=14.9$ kcal/mole which is in good agreement with the present result.

The parameters determined for the rate limiting step in the desorption process are unusual. The preexponential factor, $A=2.5 \times 10^{10} \text{ sec}^{-1}$, is within the range of preexponential factors for a surface diffusion step, which is expected to be in the range of $10^{10}-10^{12} \text{ sec}^{-1}$.¹⁴ It may be that the rate limiting step is diffusion to an active site followed by desorption. However, the activation energy, $E_d=15.4$ kcal/mole, is quite high for diffusion.

The activation energy is more consistent with desorption as the rate limiting step. There is some theoretical disagreement on the values for preexponential factors for desorption; however, they are generally considered to be in the range of 10^{12} to 10^{18} sec^{-1} .^{15,16} It is not clear how the preexponential factor might change if the ammonia were adsorbed in some complex manner to the surface. For example, the ammonia may be bound through the nitrogen with additional weak binding of one or more of the hydrogen atoms to neighboring platinum atoms.

B. The kinetics of ammonia decomposition on the stepped Pt(557) surface.

The Pt(557) surface is approximately 16 times more reactive in ammonia decomposition than the low index (111) face, affording easier study of the mechanisms of decomposition.

Our model for the mechanisms of ammonia scattering and decomposition, if successful, must explain the following experimental observations

obtained for this complex reaction on the Pt(557) crystal face.

a. The temperature dependent behavior of the decomposition probability, with ammonia adsorption-desorption to around 500 K, increased probability of decomposition above 500 K to around 800 K, and declining decomposition probability at higher temperatures.

b. The first-order dependence in incident beam intensity on the decomposition probability,

c. The large phase lags observed for the H₂ and N₂ product signals at lower temperatures,

d. The first-order behavior in incident beam intensity for the H₂ signal phase lag and the higher order dependence for the N₂ signal phase lag.

First the temperature behavior of the decomposition reaction is unusual. Previous studies of ammonia decomposition on platinum had generally shown a monotonic increase of reactivity with increasing temperature, with the exception of certain samples used by Robertson and Willhoft.¹⁷⁻¹⁹ Unfortunately, they could not establish their sample conditions by any analytical technique. Due to the slow self-poisoning of the decomposition reaction it is possible that the decomposition behavior observed here would not be found at higher ammonia pressures.

At low temperature (350-500 K) there are large changes in NH₃ amplitude and a sharp maximum in ammonia phase lag similar to the behavior on the Pt(111) surface, indicative of significant adsorption and subsequent rate limiting desorption. Although there is substantial adsorption, there is no indication of decomposition in this low temperature range. In the second region (500-800 K) the H₂ production increases with the simultaneous

fall in amplitude for the scattered, unreacted ammonia. The H_2 production reaches a maximum at approximately 700 K at which point approximately 18% of the incident ammonia decomposes. This behavior could be modeled by a branch mechanism with desorption predominating at low temperature, and the decomposition branch becoming significant and perhaps predominant at the higher temperatures.

In the high temperature region the decomposition probability declines, reaching 1% or less of the incident ammonia at 1250 K. Three mechanisms which could account for the decline in decomposition products and simultaneous rise in the scattered unreacted NH_3 signal are an additional desorption branch, a temperature dependent sticking coefficient, and a failure of the adsorbed ammonia to fully equilibrate with the platinum surface. These models are discussed in greater detail in the appendix.

The decomposition probability is first order in incident beam intensity (Figure 12) which implies that mechanisms affecting adsorbed molecular ammonia must be first-order. Or, specifically, there cannot be higher order interactions between adsorbed ammonia states which are capable of desorbing or between adsorbed ammonia states and intermediates or products.

Assuming the steps are active sites for decomposition, it is necessary to determine if diffusion from terraces to the steps is significant. The large phase lags for N_2 and H_2 product signals (Figure 10) indicate that the decomposition is slow. If there is diffusion to the steps, competition for active sites should lead to a decline in the decomposition probability for higher surface concentration. Since the decomposition probability is linear in beam intensity, it appears that diffusion is not important to

first approximation.

Figure 10b shows large phase lags for N_2 and H_2 for temperatures below 800 K and 700 K, respectively. The N_2 phase lags are greater than the H_2 phase lags, indicating a longer surface residence time before the appearance of N_2 in the gas phase. The N_2 signal phase lags become greater than 90° , so there must be more than one slow step in the pathway of N_2 formation via the decomposition of ammonia and its desorption from the surface. The H_2 signal phase lag is essentially independent of beam intensity, as shown in Figure 11, which implies that the rate determining step in the H_2 pathway must be one that is first order.

It is likely that atomic diffusion leading to recombination and desorption is one of the steps in the H_2 production pathway. The hydrogen recombination and desorption process has been measured in this laboratory.²⁰ The times measured for recombination and desorption were much shorter than the H_2 production times from ammonia measured here which suggests that hydrogen diffusion, recombination, and H_2 desorption should be relatively fast steps in the H_2 production pathway.

The N_2 phase lag (Figure 12) shows definite higher order effects. Therefore, there must be a slow higher order step in the N_2 production along with any first order steps. We have assumed that the higher order step is N_{ads} diffusion and recombination.

Three basic reaction model mechanisms were tried with a number of lesser modifications to each one to give altogether 10 model mechanisms. Figure 15 gives the model (Model A) that best fits the experimental data. The kinetic parameters (rate constants, preexponential factors, and activation energies) that were calculated for this complex branched model are

listed in the figure. The scattered ammonia signal amplitude and phase lag data and the product H_2 amplitude and phase data are compared to the behavior predicted by reaction model mechanism A in Figures A2a-c and A3a-c, respectively, in the appendix. The fit, which is qualitatively correct, has several quantitative discrepancies, but model A is the most probable of the several models that we have tried. Possible causes for the quantitative discrepancies and their implications are discussed in the appendix along with a description of the less successful models.

In spite of the quantitative discrepancies, the model of Figure 15 demonstrates that incorporation of the points discussed here in a reaction model mechanism can yield qualitative agreement with the data.

The models discussed do not directly address the hydrogen-deuterium isotope exchange in the adsorbed ammonia, or the source of poisoning of the ammonia decomposition. In the hydrogen-deuterium isotope exchange, /all deuterated species were detected. The peak in the exchanged species signal amplitudes occurred near 675 K. The phase lag in the $m/e=20$ signal increases rapidly for temperatures less than 600 K. It appears that the decline in amplitude at low temperatures is due to long surface residence times and dephasing. At high temperatures the exchange probability might decline due to shorter residence times of NH_3 and D_2 or due to eventual decomposition of the exchanged species. It seems unlikely that the exchange is proceeding through partial dissociation and recombination. Any partial dissociation would release free adsorbed hydrogen. Since hydrogen surface diffusion is believed to be fast,²¹ // partial dissociation would presumably lead to H_2 production. Yet at 500 K there is significant exchange and essentially no H_2 production. Hence, it appears that hydrogen-deuterium exchange occurs through an interaction of adsorbed ammonia molecules and

surface deuterium atoms, perhaps through the formation of intermediate Pt-NH₃D species.

The cause of the poisoning could not be determined. It slowly inhibited ammonia decomposition, and the rate of poisoning seemed highest at the temperatures where the decomposition probability was greatest. After poisoning the activity of the surface could be restored by heating the crystal in vacuum for approximately three minutes at 1200 K. Auger spectroscopy failed to show any detectable chemical contamination on the poisoned surface. Flash desorption from the poisoned surface occasionally showed a barely detectable strongly bound peak at mass 28, and occasionally a much smaller peak at mass 14; however, the peaks were not consistently reproducible. The inhibition of the decomposition reaction could result from formation of a small amount of strongly bound nitrogen at the active sites. However, its formation would involve a small fraction of the NH₃ molecules at most and, except for the slow inhibition observed, would not be a significant part of the ammonia interaction. Melton and Emmett²² found that in contrast to ammonia adsorption on iron, ammonia adsorption on platinum yields only a small amount of strongly bound nitrogen containing species.

Conclusion

There is evidence that ammonia adsorbs associatively on the (111) and (557) single crystal faces of platinum, the adsorption occurring with a large sticking coefficient (.74 on Pt(111), and .54 on Pt(557)). Adsorption leads to subsequent desorption or decomposition with final

decomposition products N_2 and H_2 . We have found that the (557) crystal face is approximately 16 times more reactive for ammonia decomposition than the (111) face, presumably due to the higher density of steps. Increased reactivity of stepped surfaces has been observed previously, for instance, in some hydrocarbon reactions²³ and in dissociative hydrogen adsorption.^{5,24}

From kinetic model fit to the data we have found that the activation energy for the desorption process on the (111) surface is $E_d=15.4$ kcal/mole with a preexponential $A=2.5 \times 10^{10} \text{ sec}^{-1}$.

For ammonia scattering from the Pt(557) surface, the probability for decomposition to nitrogen and hydrogen is near zero below 500 K, increases steadily to approximately .18 at 750 K, then declines steadily towards zero up to 1200 K, which is the highest temperature investigated.

The Pt(557) decomposition data show that the decomposition probability is first order in incident ammonia, from which we conclude that the initial decomposition steps are first order. There are slow higher order steps in the pathway leading to N_2 production, but any higher order steps in the H_2 production pathway are fast compared to the first order steps.

Several models have been suggested to describe the kinetics of ammonia scattering and decomposition on the Pt(557) surface. Some of the models agree qualitatively with the data, but none of the models quantitatively reproduce the observed kinetics. The models are described in the appendix.

Acknowledgement

This work was supported by the National Science Foundation, and by the Division of Materials Sciences, Basic Energy Sciences, U.S. Department of Energy.* We thank Professor D.R. Olander for providing a copy of his least squares fitting routine, and T.H. Lin for assistance on some of the experiments.

*Under Contract #W-7405-ENG-48

References

1. W.G. Frankenburg, Catalysis, P.H. Emmett, ed., Rheinhold Publishing Corp., New York (1955) v.3, p.171.
2. R.J. Madix and J.A. Schwarz, Surface Sci. 24, 264 (1971).
3. R.H. Jones, D.R. Olander, W.J. Siekhaus, and J.A. Schwarz, J. Vac. Sci. Technol. 9, 1429 (1972).
4. S.L. Bernasek and G.A. Somorjai, J. Chem. Phys. 62, 3149 (1975);
R.J. Gale, Ph.D. Thesis, University of California, Berkeley, 1978;
S.L. Bernasek, Ph.D. Thesis, University of California, Berkeley, 1975.
5. M. Salmeron, R.J. Gale, and G.A. Somorjai, J. Chem. Phys. 67, 5324 (1977).
6. D. Auerbach, C. Becker, J. Cowin, and L. Wharton, Proceedings of the VI Intl. Symp. on Molecular Beams, Noordwijkerhout, Netherlands, 1977.
7. Of the many studies that have observed coverage dependent sticking coefficients, most have used AES, work function measurements, or flash desorption to determine the extent of adsorption, thus the sticking coefficient measured is that for extended time adsorption, several seconds to minutes. One example of coverage dependent sticking coefficient determined by molecular beam techniques is
T. Engle, J. Chem. Phys. 69, 373 (1978).
8. C.T. Foxon, M.R. Boudry, and B.A. Joyce, Surface, Sci. 44, 69 (1974).
9. J.A. Schwarz and R.J. Madix, Surface Sci. 46, 317 (1974).
10. D.R. Olander and A. Ullman, Intl. Journal of Chem. Kinetics 8, 625 (1976).
11. H.-C. Chang and W.H. Weinberg, Surface Sci. 72, 617 (1978).
12. MINUIT minimization program adapted for modulated beam-surface scattering by D. Dooley and D.R. Olander from the special library at Lawrence Berkeley Laboratory.
13. J.L. Gland, Surface Sci. 71, 327 (1978).
14. R.C. Baetzold and G.A. Somorjai, J. Catal. 45, 94 (1976).
15. G. Armand, Surface Sci. 66, 321 (1977).
16. H. Ibach, W. Erley, and H. Wagner, Surface Sci. 92, 29 (1980).

17. C.E. Melton and P.H. Emmett, J. Phys. Chem. 68, 3318 (1964).
18. D.G. Löffler and L.D. Schmidt, Surface Sci. 59, 195 (1976).
19. A.J.B. Robertson and E.M.A. Willoft, Trans. Far. Sco. 63, 476 (1967).
20. M. Salmeron, R.J. Gale, and G.A. Somorjai, J. Chem. Phys. 70, 2807 (1979).
21. K. Christman and G. Ertl. Surface Sci. 60, 365 (1976).
22. C.E. Melton and P.H. Emmett, J. Phys. Chem. 68, 3318 (1964).
23. D.W. Blakely and G.A. Somorjai, J. Catal. 42, 181 (1976);
J.L. Gland, K. Baron, and G.A. Somorjai, J. Catal. 36, 305 (1975).
24. S.L. Bernasek and G.A. Somorjai, J. Chem. Phys. 62, 3149 (1975).

Figure Captions

- Fig.1 Schematic of the molecular beam scattering apparatus.
- Fig.2 Integral mode amplitude and phase lag of N_2 scattered from hot (1200 K) platinum surface as a function of incident N_2 chopping frequency. Solid lines are behavior predicted by simple model (Eq. 1 of text).
- Fig.3 Models of Pt(557) and Pt(111) crystal surfaces.
- Fig.4 Integral mode amplitude and phase lag of ammonia scattered from the Pt(111) surface as a function of crystal temperature. Curves are best fit to simple adsorption-desorption model. (a) $f=5$ cps, (b) $f=20$ cps, (c) $f=50$ cps, (d) $f=150$ cps.
- Fig.5 H_2 production from ammonia on the Pt(111) surface. Integral mode normalized amplitude and phase lag as a function of crystal temperature. (a) amplitude, (b) phase lag.
- Fig.6 Angular distribution of ammonia scattered from Pt(111) surface. Amplitude of differential mode signal for a chopping frequency, $f=100$ cps. (a) $T_{Xtal}=1250$ K, (b) $T_{Xtal}=375$ K.
- Fig.7 Ammonia sticking coefficient $(1-r_{375K}/r_{1250K})$ on Pt(111) as a function of incident beam intensity. The integral mode scattered ammonia amplitude for a crystal temperature of 1250 K is used to measure incident beam intensity. $f=150$ cps.
- Fig.8 ND_3 ($m/e=20$) product amplitude from scattering of a mixed beam of NH_3 and D_2 from a Pt(111) surface. Differential mode, detector at surface normal.
- Fig.9 Integral mode amplitude and phase lag of ammonia ($m/e=17$) scattered from the Pt(557) surface as a function of crystal temperature. (a) $f=5$ cps, (b) $f=20$ cps. (c) $f=50$ cps.
- Fig.10 Integral mode amplitude and phase lag for H_2 and N_2 product signals as a function of crystal temperature. The chopping frequency of the incident ammonia beam is 5 cps. (a) amplitude, (b) phase lag.
- Fig.11 Ammonia beam intensity dependence of hydrogen and nitrogen phase lags. Signal phase lag at a crystal temperature of 725 K are plotted as a function of the scattered ammonia amplitude at 1250 K, $f=5$ cps.

- Fig.12 Ammonia beam intensity dependence of hydrogen, nitrogen, and ammonia signal amplitudes. Signal amplitudes measured at $T_{\text{Xtal}}=725$ K are plotted in unnormalized, arbitrary units. Lines are linear least squares fit to the data.
- Fig.13 ND_3 ($m/e=20$), ND_2H ($m/e=19$), and NDH_2 ($m/e=18$) normalized product signal amplitudes from scattering of a mixed beam of NH_3 and D_2 from Pt(557) surface. The signals were measured in the differential mode; the detector was placed at the surface normal. The NDH_2 signal is corrected by subtracting the expected contribution from ND_3 and ND_2H . $f=5$ cps.
- Fig.14 Crystal temperature dependence of ammonia adsorption, decomposition, and isotope exchange (from NH_3+D_2) on Pt(557). Ordinate is signal amplitude in arbitrary units. Curves have been drawn through the data points to assist the eye.
- Fig.15 Homogeneous reaction model. This model gave the best agreement to the data. The rate constants are those which corresponded to the minimal value in the least squares fit.
- Fig.A1. Reaction models for the decomposition and scattering of NH_3 on Pt(557); (a) homogeneous model making no distinction between terraces and steps, (b) heterogeneous separation of surface into sites near and far from steps, (c) temperature dependence in the sticking coefficient s for a homogeneous model, (d) and (e) example non-first order decomposition mechanisms.
- Fig.A2. $\text{NH}_3/\text{Pt}(557)$. Integral mode ammonia signal amplitude and phase lag. The curves are the best fit to the data for the reaction model shown schematically in Figure 15.
- Fig.A3. $\text{NH}_3/\text{Pt}(557)$. Integral mode H_2 signal amplitude and phase lag. The curves are the best fit to the data for the reaction model shown schematically in Figure 15.

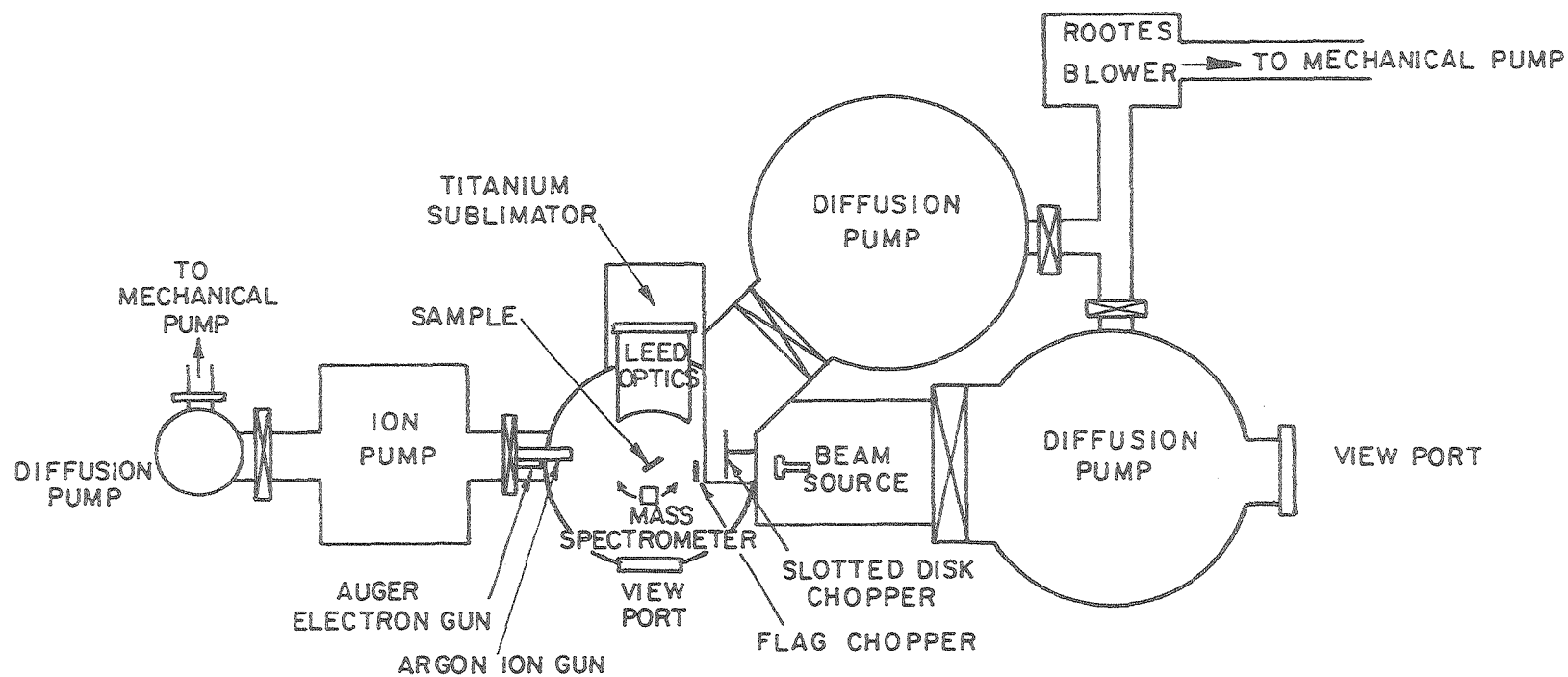
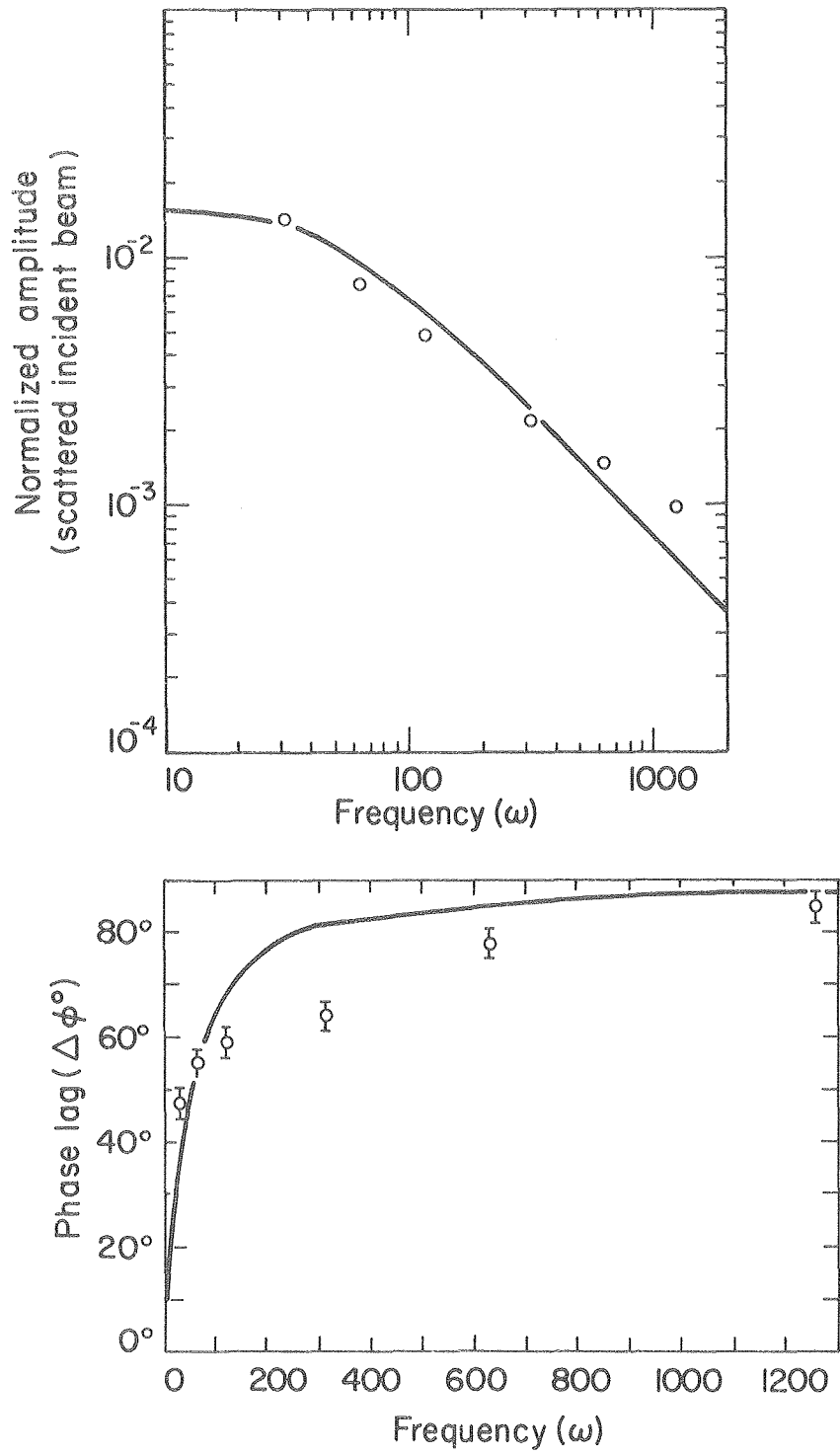


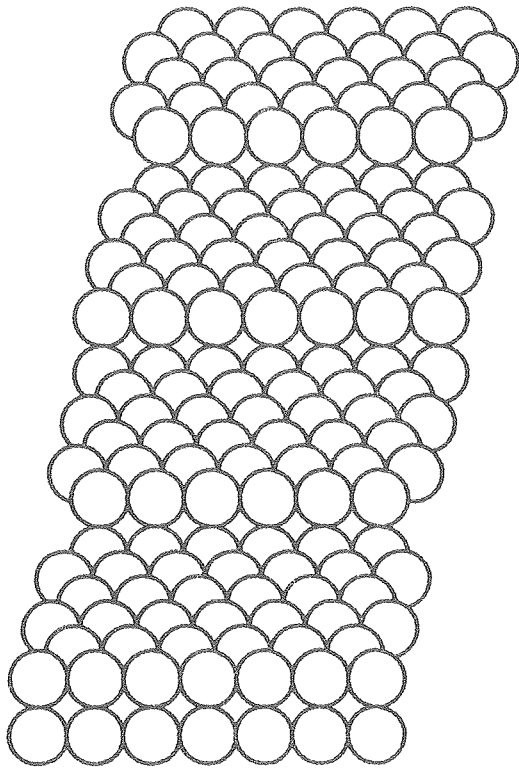
Fig. 1

XBL 785-4948

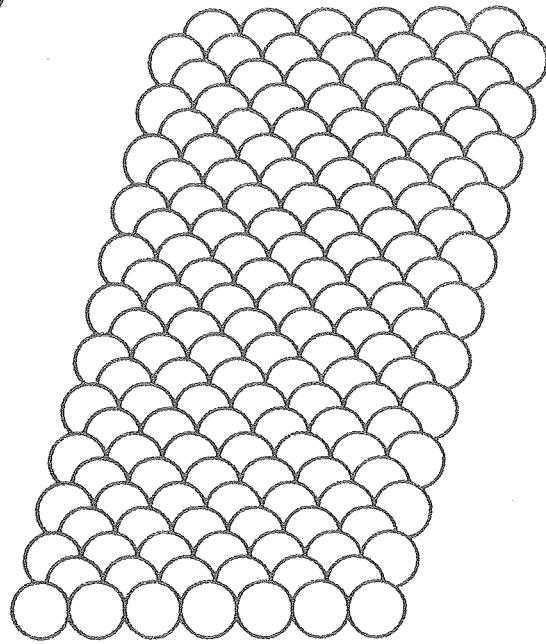


XBL 798-2533

Fig.2



Pt (557)



Pt (111)

XBL 8011-12082

Fig.3

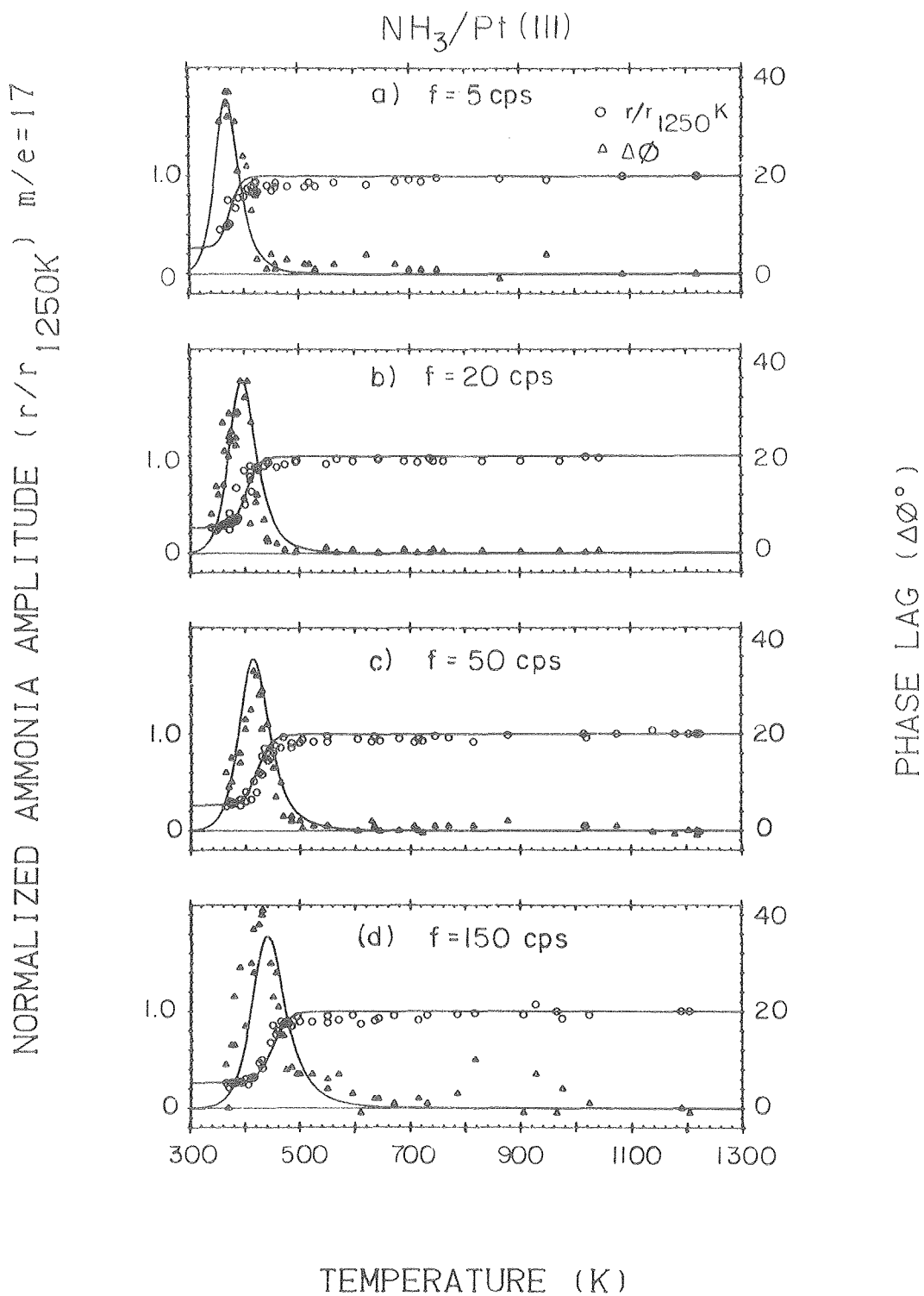
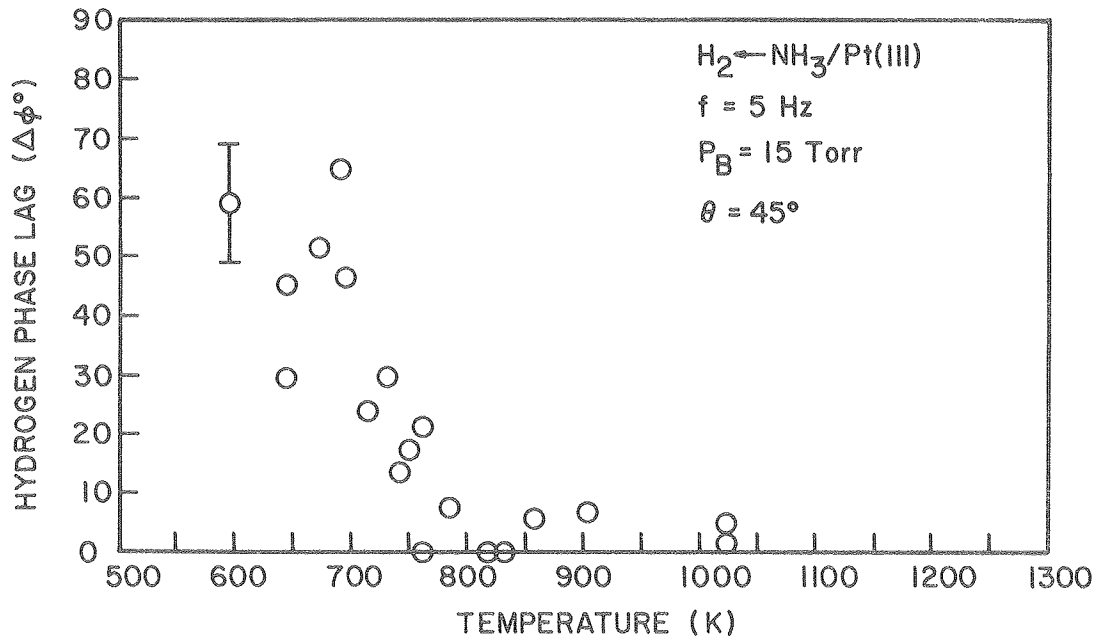
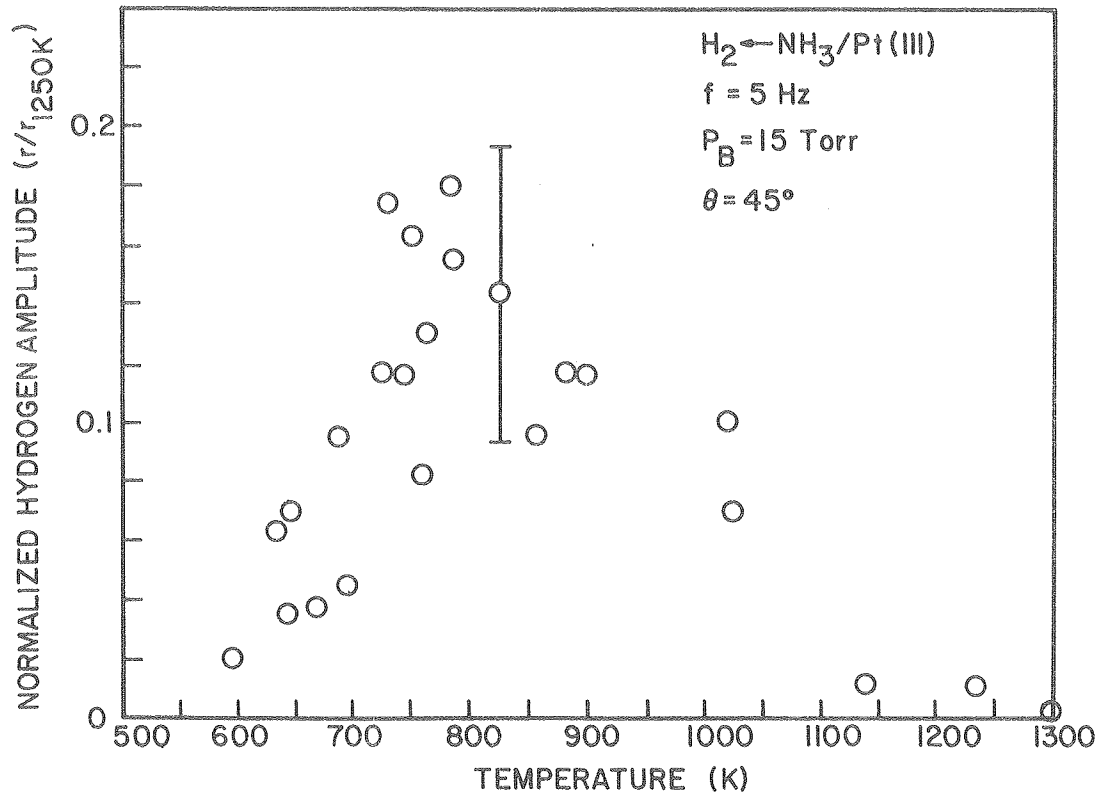
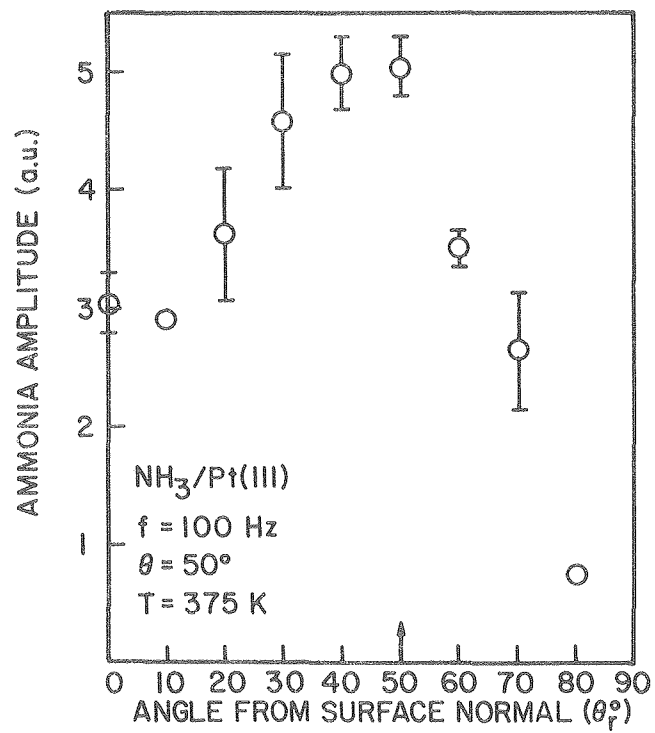
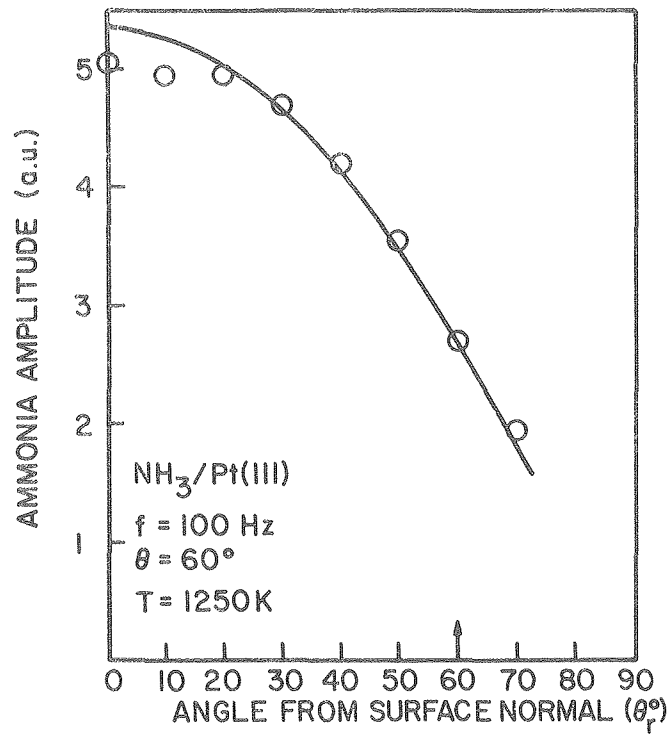


Fig.4



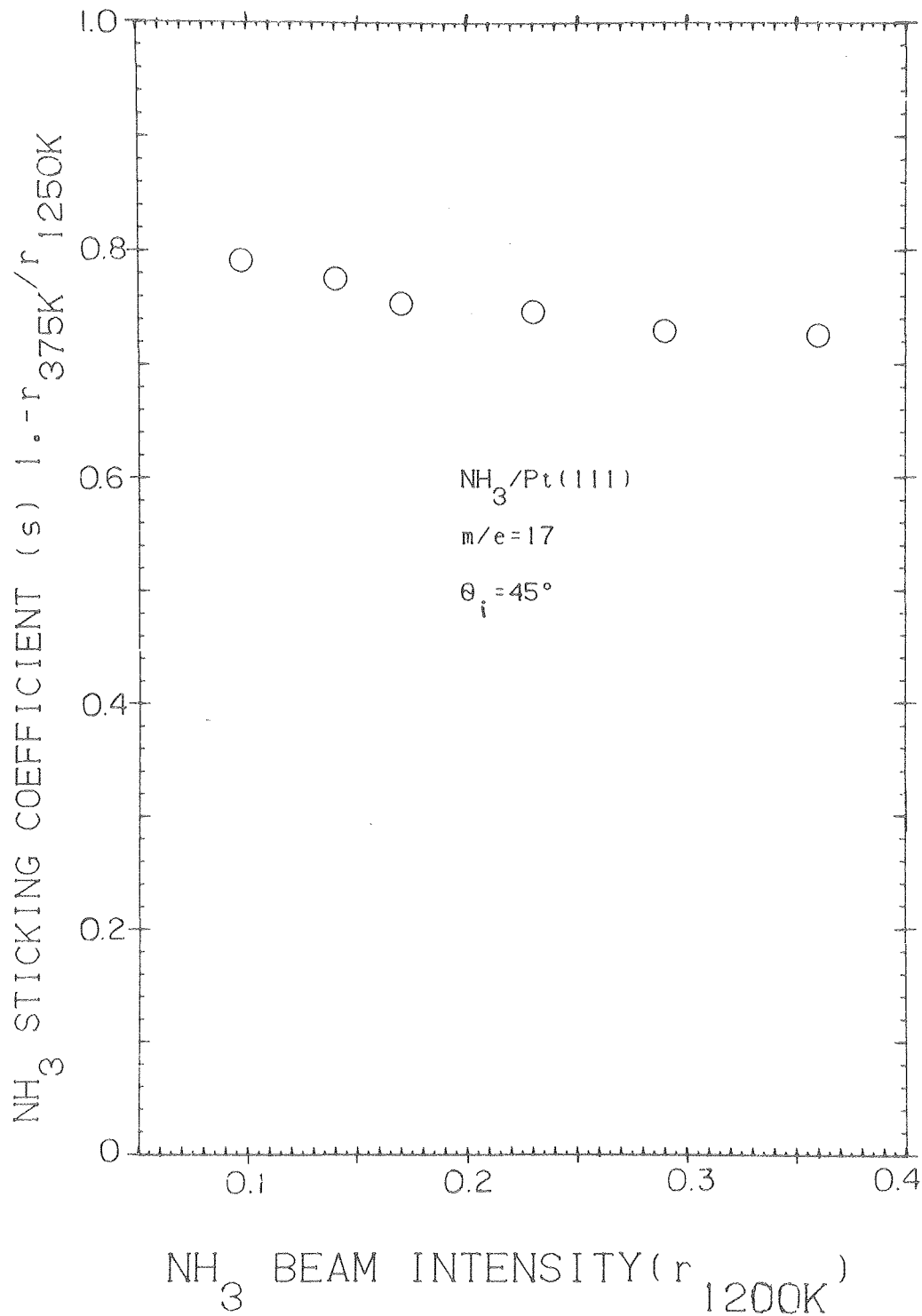
XBL 798-11049

Fig.5



XBL 798-11048

Fig.6



XBL 808-10989A

Fig.7

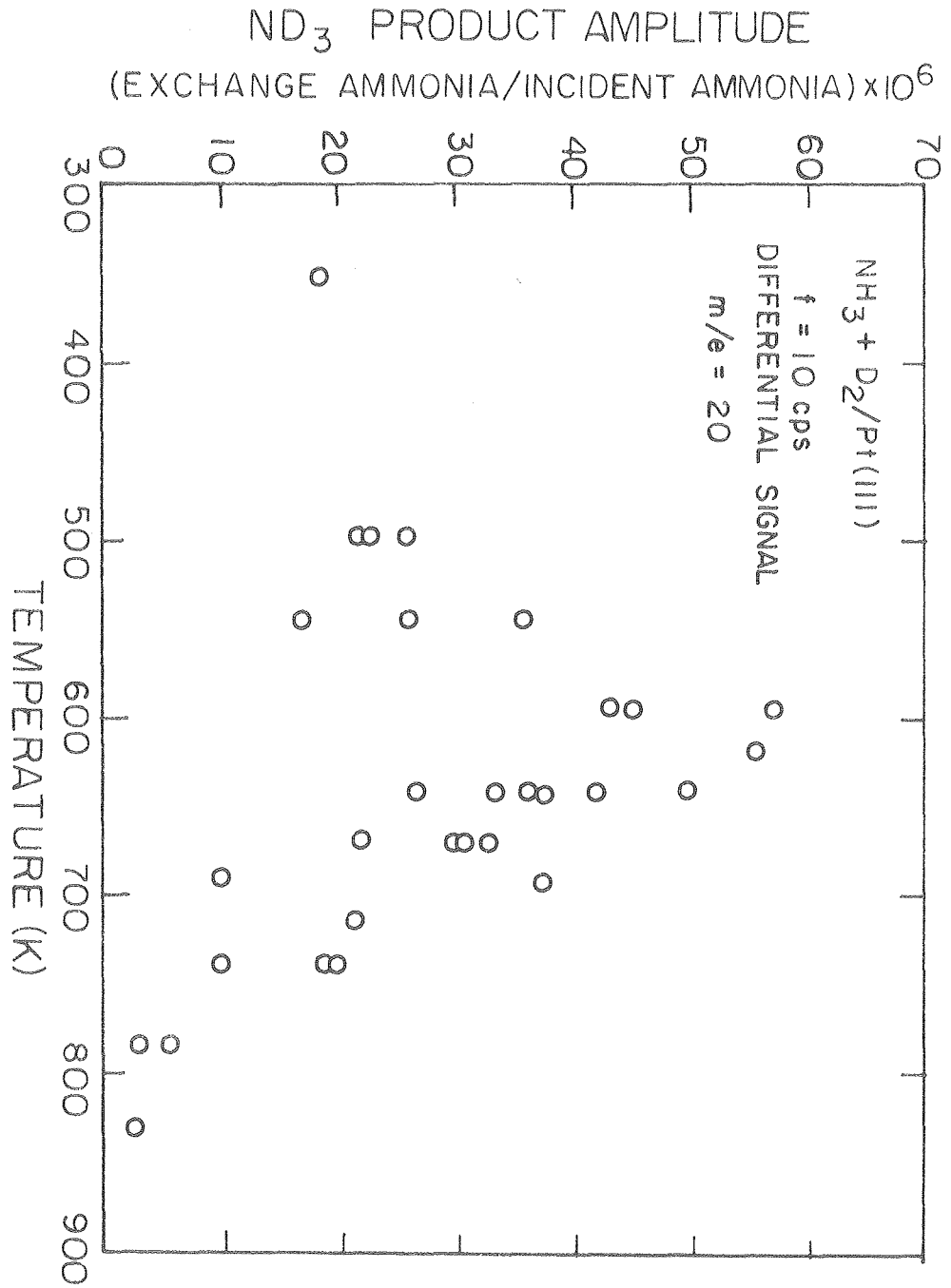
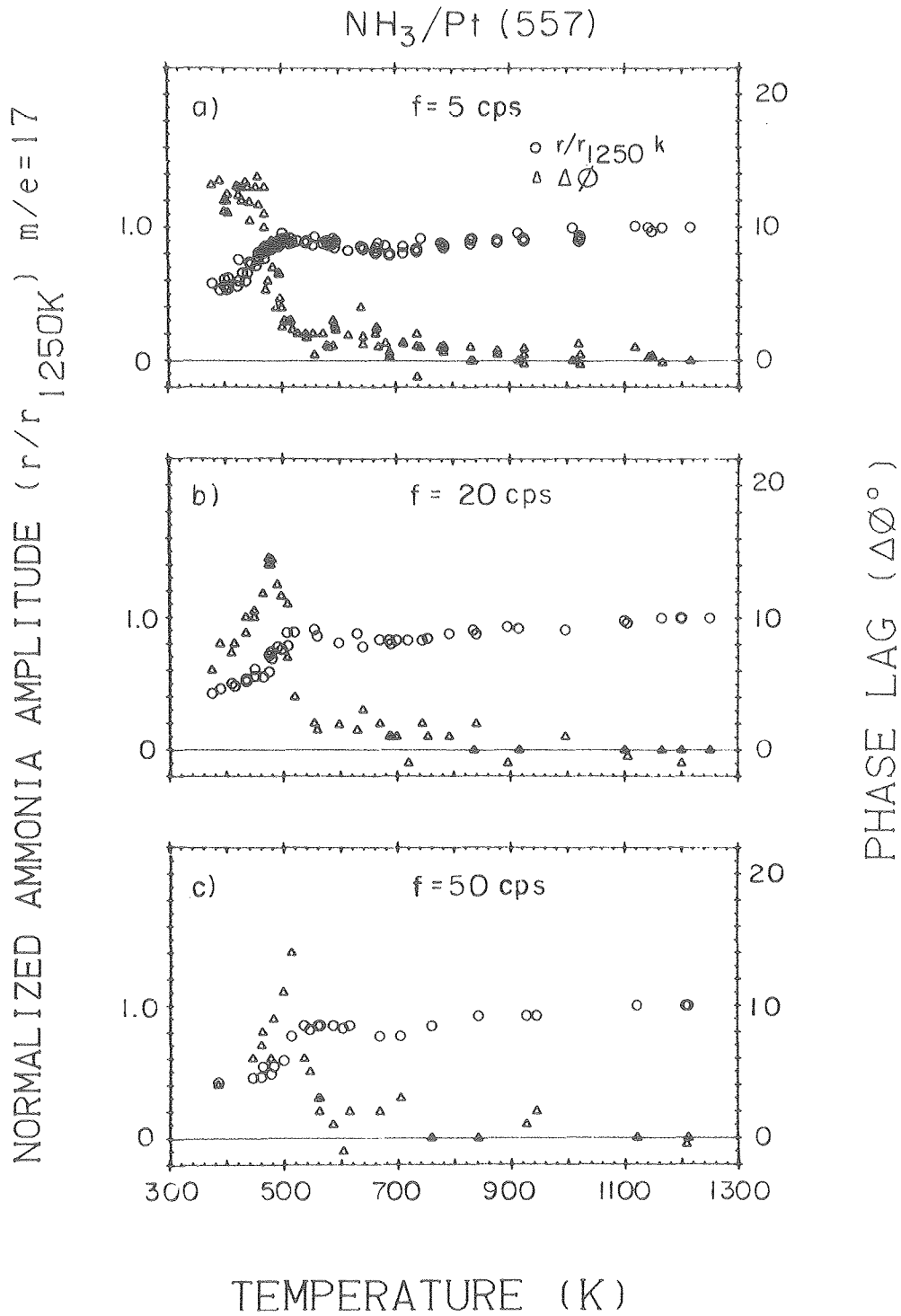
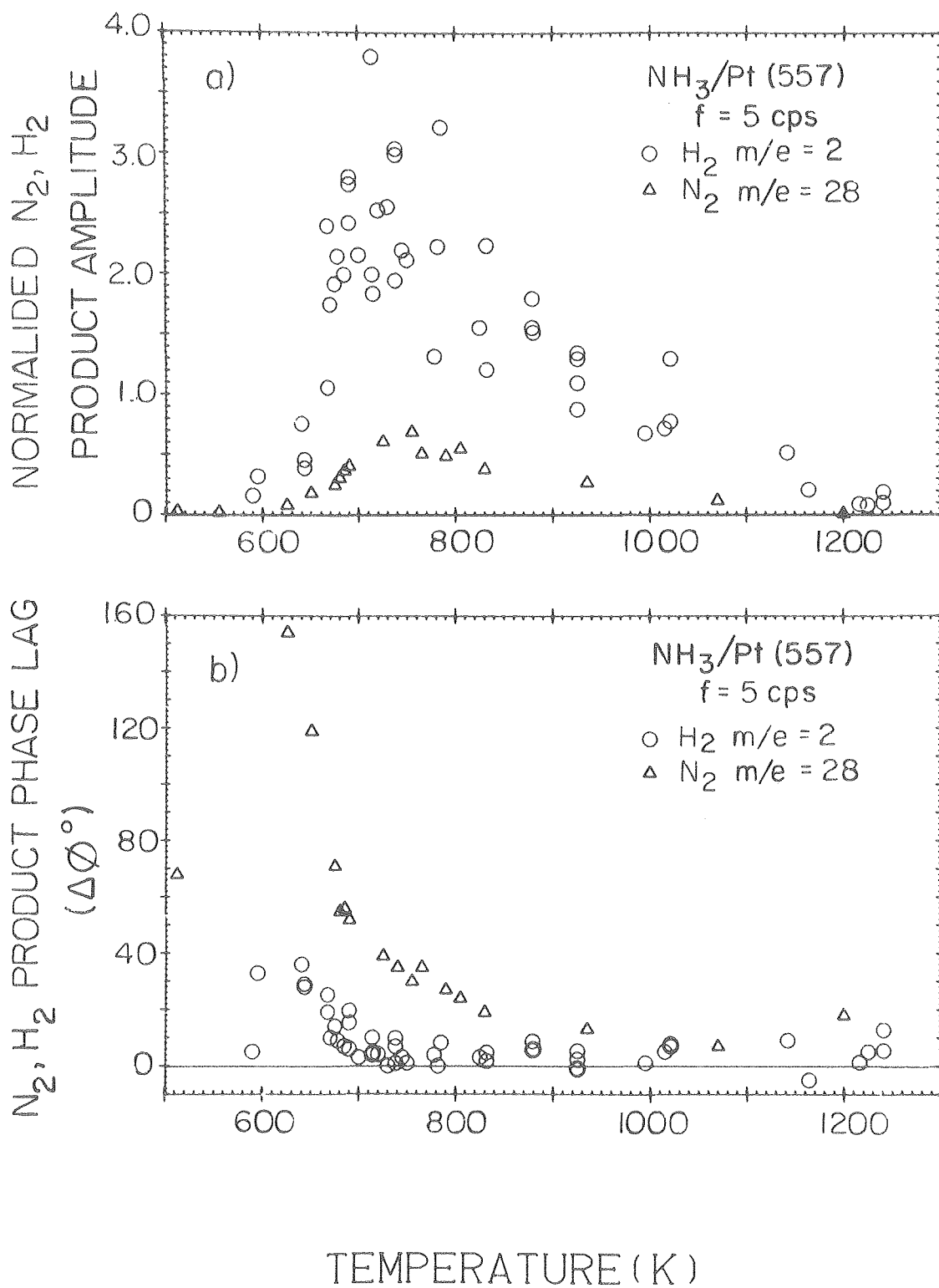


Fig.8



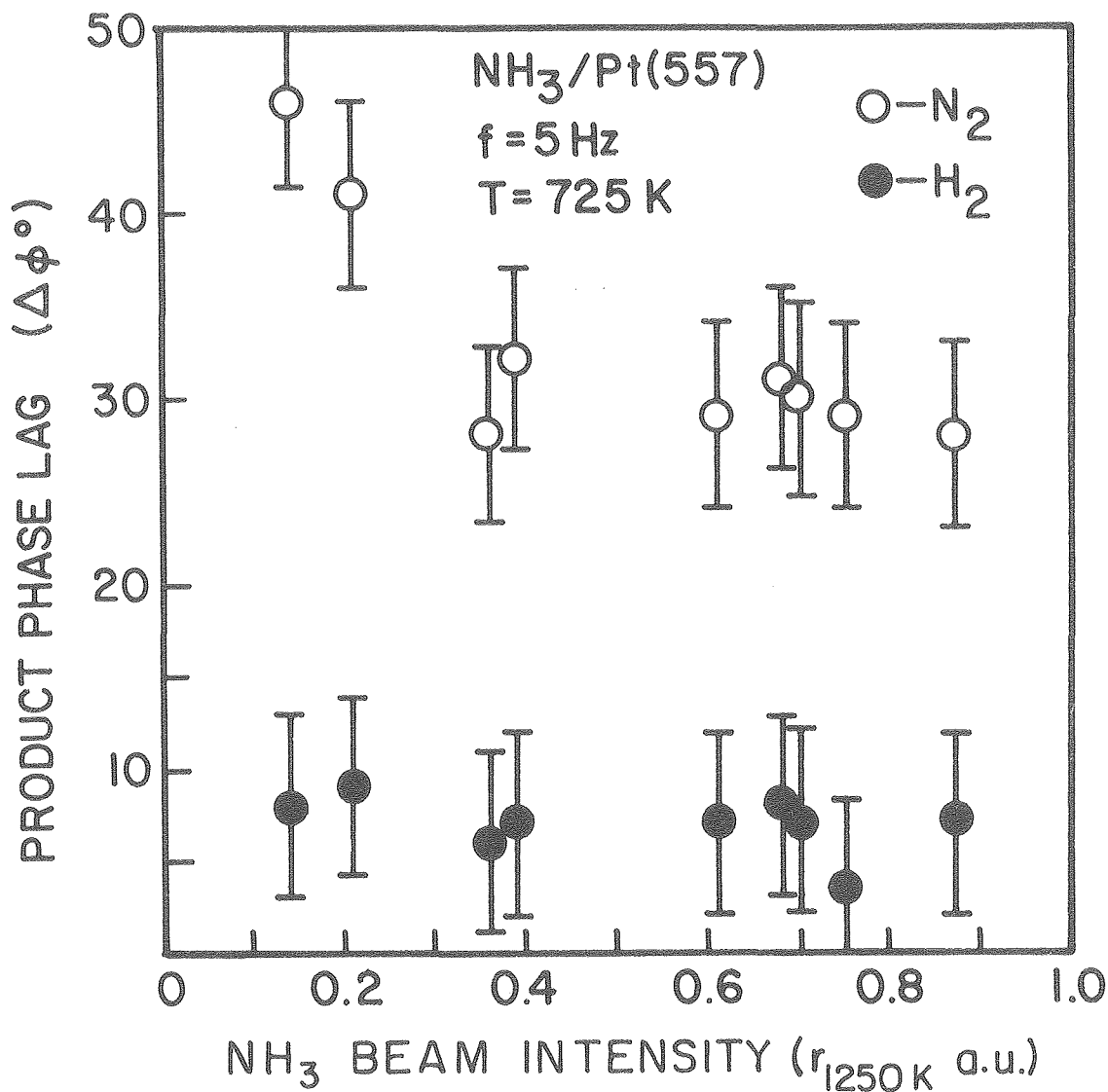
XBL8011-6348

Fig.9



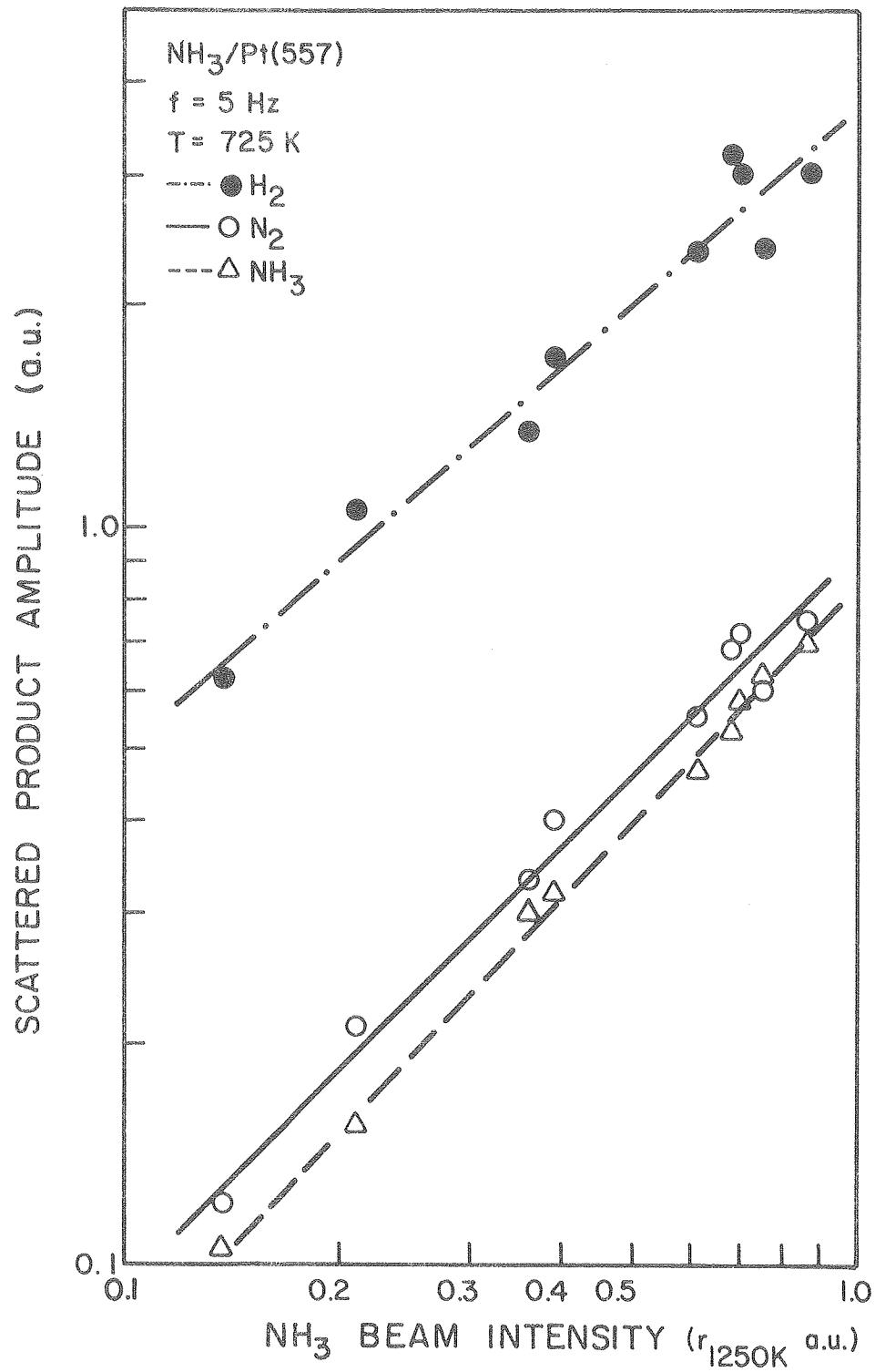
XBL 808-10987 A

Fig.10



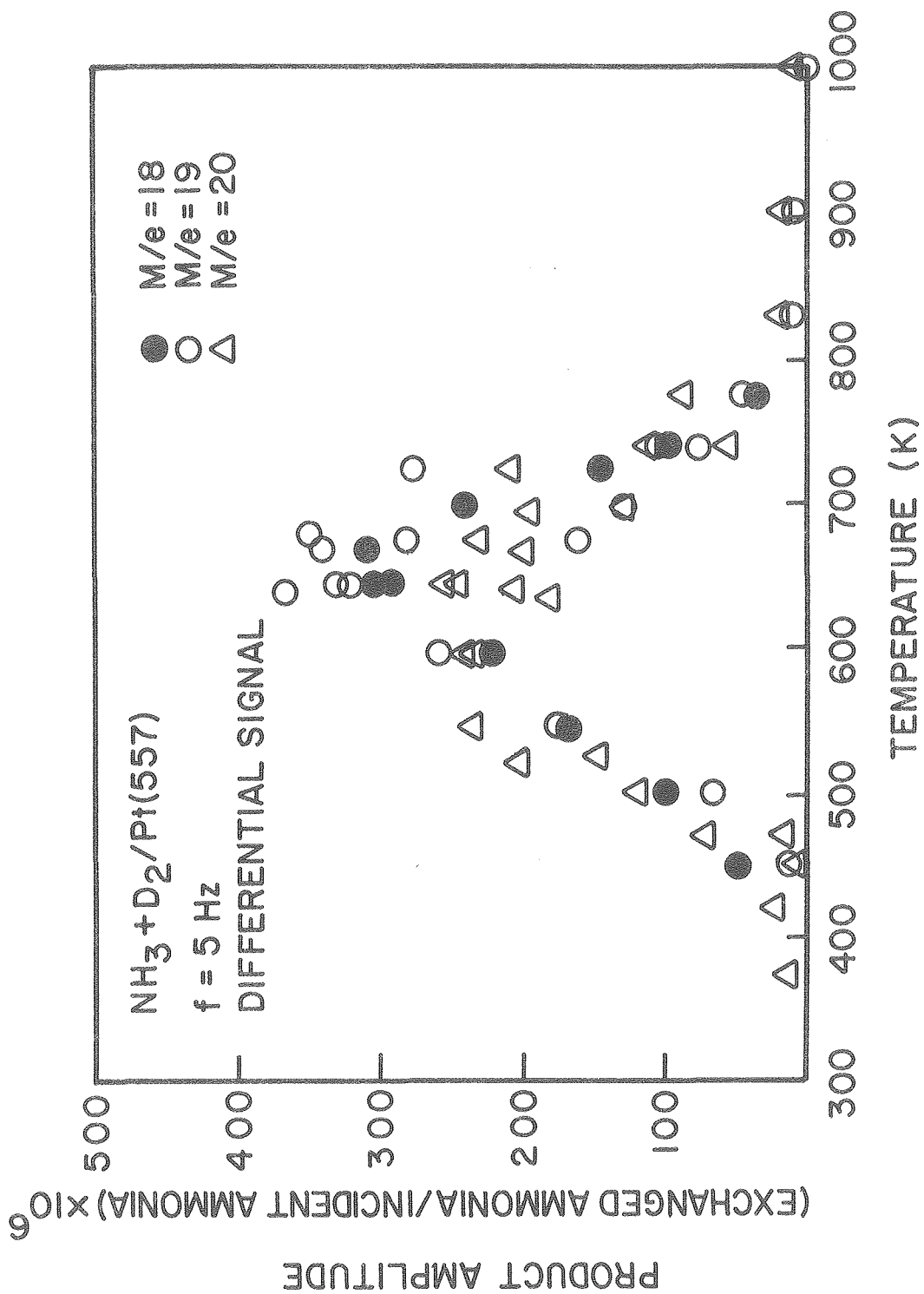
XBL 798-11045A

Fig.11



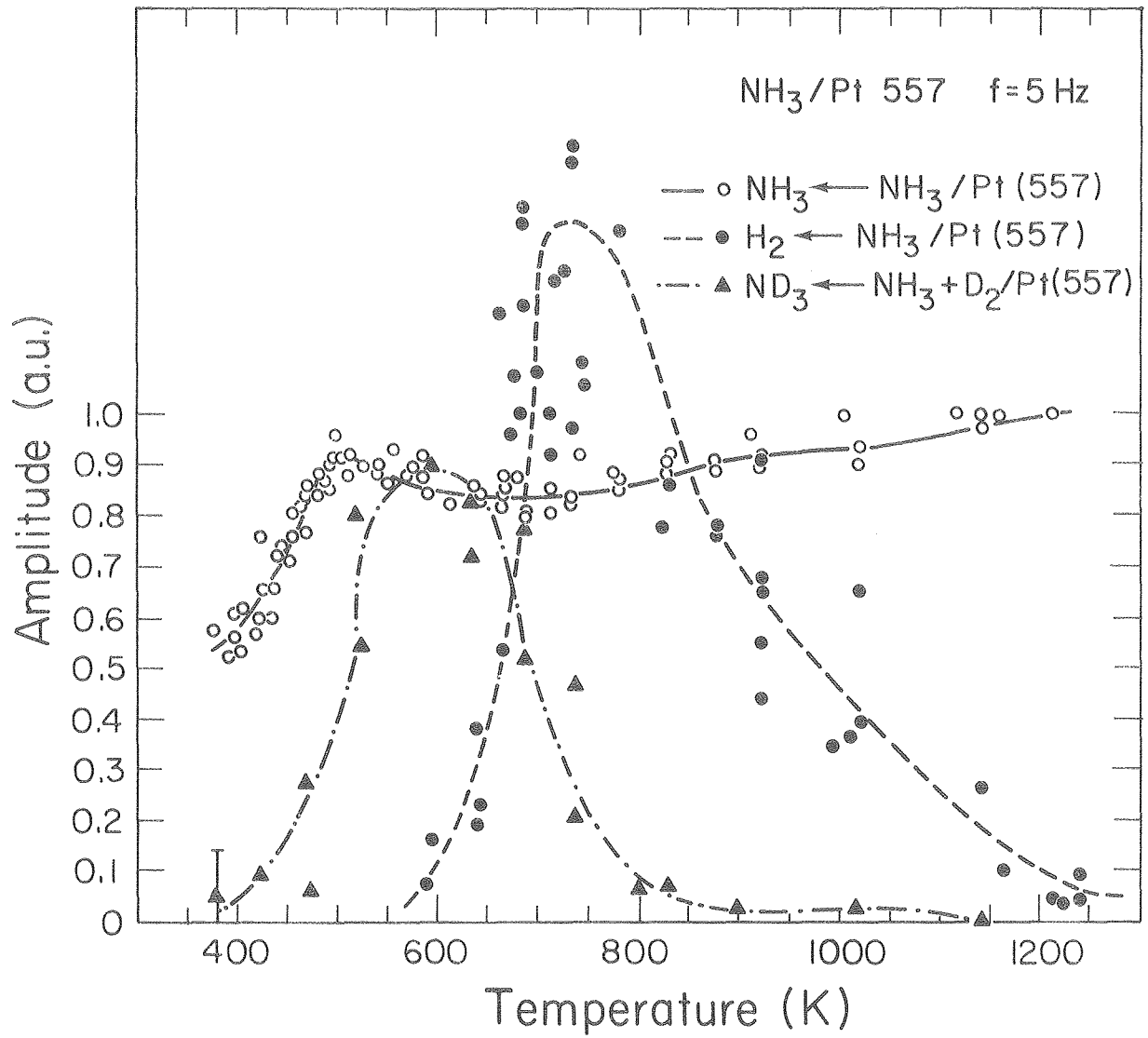
XBL 798-11044A

Fig.12



XBL 798-11046

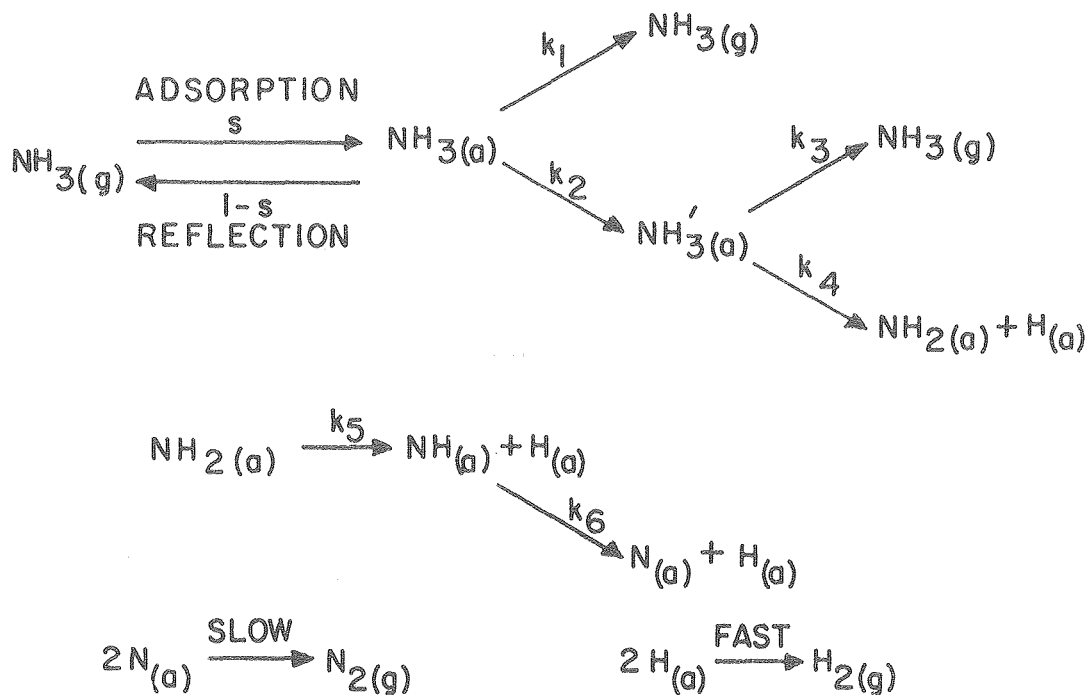
Fig.13



XBL 798-2530

Fig.14

A



$$s = 0.54$$

$$k_1 = 1.9 \times 10^8 \exp(-13.4 \text{ KCAL/MOLE}) \text{ s}^{-1}$$

$$k_2 = 7.0 \times 10^8 \exp(-17.0 \text{ KCAL/MOLE}) \text{ s}^{-1}$$

$$k_3 = 2.2 \times 10^{17} \exp(-38.4 \text{ KCAL/MOLE}) \text{ s}^{-1}$$

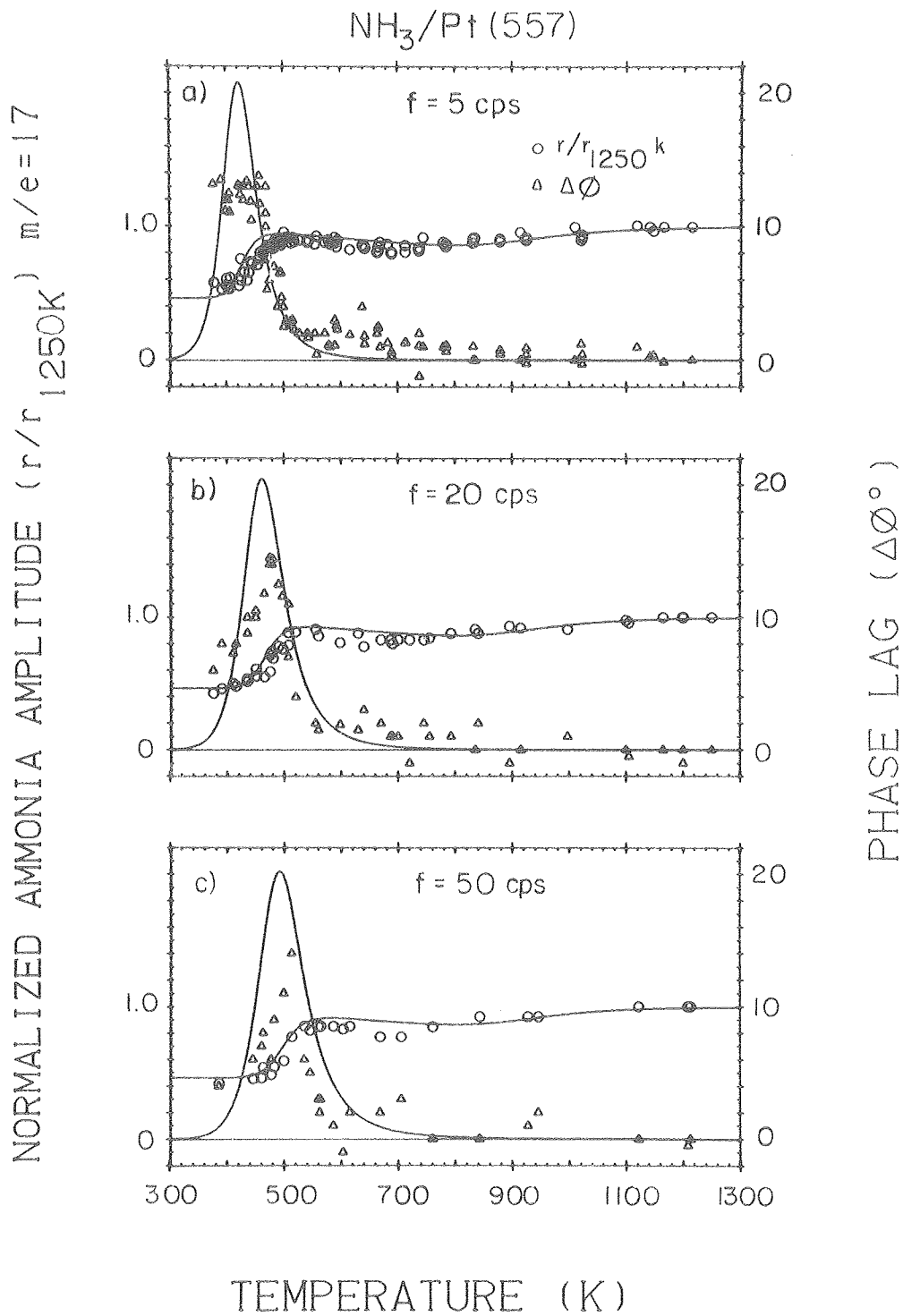
$$k_4 = 2.5 \times 10^{11} \exp(-13.3 \text{ KCAL/MOLE}) \text{ s}^{-1}$$

$$k_5 = 4.9 \times 10^8 \exp(-20.0 \text{ KCAL/MOLE}) \text{ s}^{-1}$$

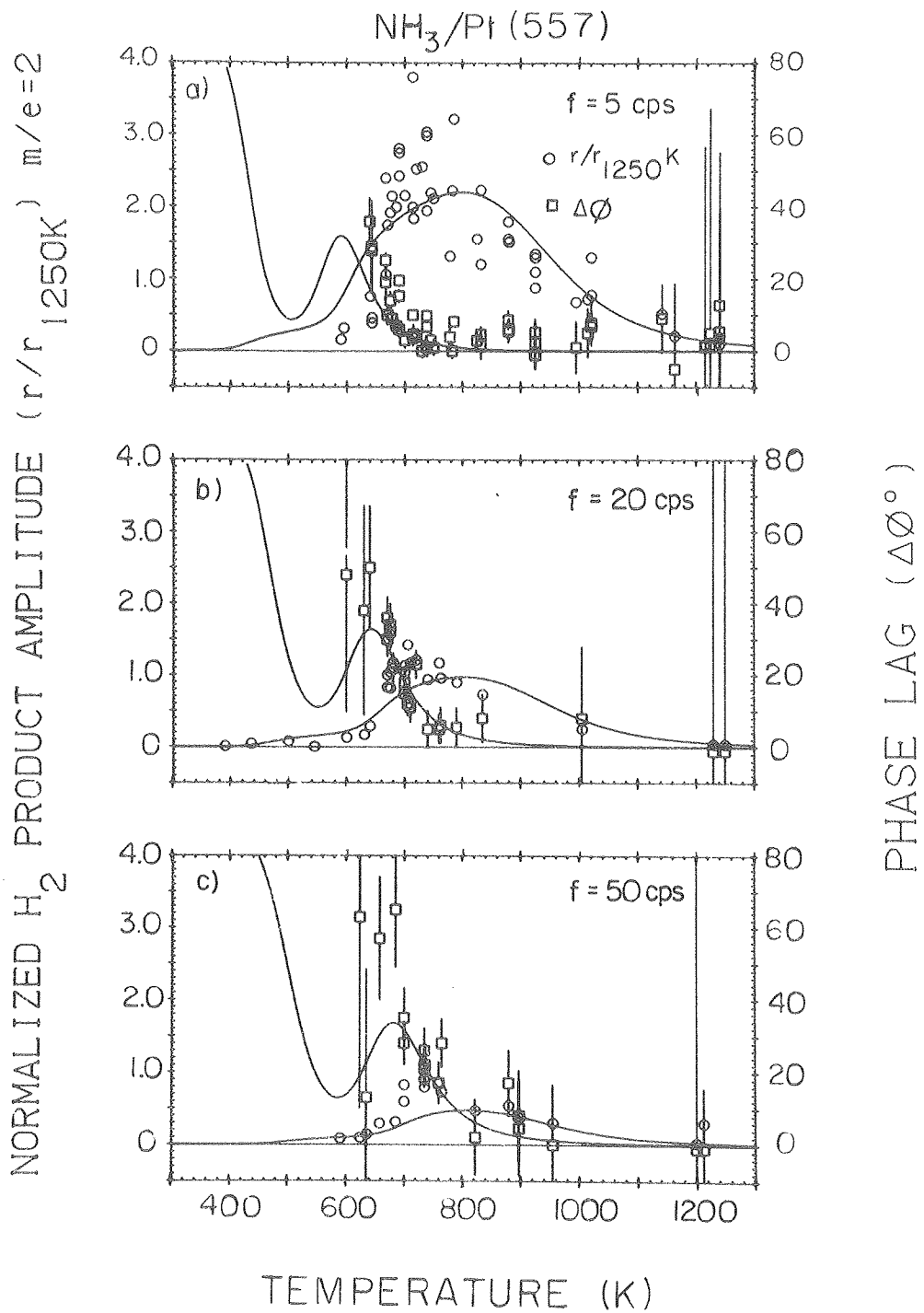
$$k_6 = 1.0 \times 10^8 \exp(-14.7 \text{ KCAL/MOLE}) \text{ s}^{-1}$$

XBL8011-6332

Fig.15



XBL 80II-6347



XBL 8011-6345

AppendixNH₃ Scattering and Decomposition on the (557) Crystal Face of
Platinum: Reaction Model Mechanisms.

Three mechanisms that could explain the temperature behavior of the probability for decomposition of ammonia on the Pt(557) surface (see Discussion above) are multiple desorption branch mechanisms, a temperature dependent sticking coefficient and a failure of the adsorbed ammonia to fully equilibrate.

Figures Ala and Alb show two examples of multiple desorption branch models for the adsorption of ammonia on the (557) surface of platinum. Model A is a homogenous model for which no distinction is made between adsorption at steps and terraces. In Model B the surface is taken to be heterogeneous and is separated into sites near surface steps and those far from steps. For simplicity, the initial desorption rates from both sites have been taken as equal. In Models A and B low temperature desorption occurs through the path k_1 . As temperature increases, path k_2 becomes predominant and initiates the decomposition. At higher temperatures k_3 stops the decomposition reaction through desorption of the ammonia. The exact details of the decomposition steps are not included in Figures Ala and Alb because of the large number of possibilities.

There is no well defined functional form for temperature dependence in the sticking coefficient so we have modeled temperature dependent adsorption in terms of a shortlived precursor state. By starting with Model A and taking the first adsorbed ammonia state as the precursor with k_1 and k_2 extremely fast, Model C is generated. (Figure Alc) The apparent adsorption probability, s , is

$$s = s \left(1 + \frac{k_1}{k_2} \right)^{-1} = s \left(1 + A' \exp \left(- \frac{E^1}{RT} \right) \right)^{-1}$$

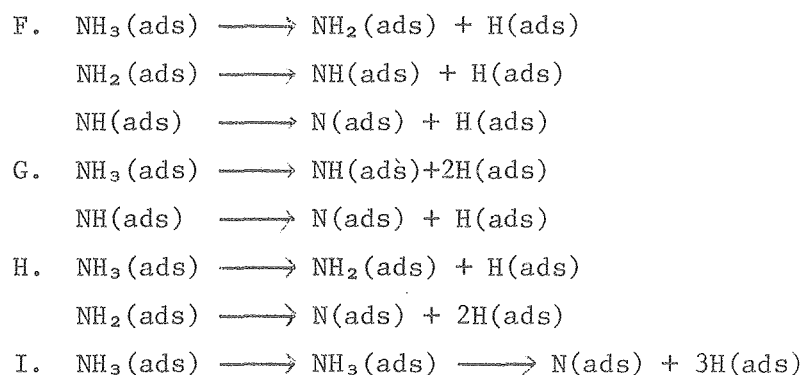
which decreases with increasing temperature.

At this point it is difficult to determine the nature of the temperature dependence if the adsorbed ammonia is not equilibrating with the surface. At higher temperatures, excitation leading to desorption might be fast enough to prevent excitation to a high enough energy level in the vibrational modes leading to decomposition. By measuring the velocity distribution of

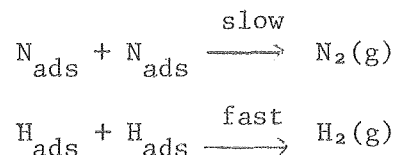
scattered ammonia we hope to investigate the question of equilibration of ammonia adsorbed on platinum. These studies are in progress in our laboratory.

Models A, B, and C are first-order in terms of molecular ammonia. They assume first order reactions on the surface and during desorption and the absence of interaction between adsorbed ammonia molecules or between adsorbed ammonia and any adsorbed decomposition product or intermediate. Models D and E (Figure A1d and A1e) are examples of potential models with higher order reactions of the various species. Models D and E are sensitive to NH_3 coverage in the decomposition range. Since the decomposition probability is first order in incident beam intensity, we conclude that Models D and E are unlikely, as are any models involving higher order interactions between surface species from which desorption of NH_3 can occur.

For the decomposition mechanism the simple mechanisms below were used,



All mechanisms F-I contain the recombination steps.



The three models A, B, and C (Figures A1a-c) were tried with the decomposition mechanisms F-I above. The model which yielded the best agreement to the data is Model A with decomposition mechanism F (Figure 15, Discussion). The scattered ammonia signal amplitude and phase lag data and the H_2 amplitude and phase data are compared to the behavior predicted by the reaction model mechanism in Figures A2a-c and A3a-c, respectively.

The heterogeneous model (Model B) with decomposition mechanism H

gave reasonable agreement with the data. The models with temperature dependent sticking coefficient (Figure A1c) gave only poor agreement with the data. As discussed below, models with decomposition mechanisms similar to I above may be more appropriate than mechanisms F, G, and H. However, the parameters for mechanism I are nearly correlated, thus the reaction model fitting program could not locate their best values.

There are a number of quantitative discrepancies between the scattering data and the predictions of the reaction model. The low temperature ammonia signal amplitude (Figure A2) is fit well. As discussed earlier with respect to scattering from the Pt(111) surface, the low temperature amplitude is determined by the sticking coefficient, s . The ammonia phase lag predicted by the model is larger than that observed. With only one active desorption branch, the phase lag depends on s , which suggests the agreement might be better with two desorption branches with different rates. Such a model was tried, but with the additional parameters, the reaction model fitting program was unable to locate a best value for the parameters.

The low temperature rise in hydrogen signal amplitude given by the reaction model is too gradual and the low temperature hydrogen phase lag is too small. In models A and B, (Figure A1) the first decomposition step must be relatively fast since it is in competition with desorption rate k_3 , and the ammonia scattering data shows that the ammonia phase lag is essentially zero in the temperature range where rate k_3 is important. If hydrogen is liberated in the first decomposition step, the competition with desorption limits the size of the hydrogen phase lag. Thus models with decomposition mechanisms similar to mechanism I above, which has an extra activation step prior to hydrogen liberation, may be more accurate than mechanisms F, G, and H.

All the models with multiple steps for liberation of hydrogen show complex behavior for the product H_2 signal phase lag as seen in Figures A3a-c. The errors in the H_2 signal phase lag data are too large and the temperature range in the data is too small to determine if the complex behavior predicted by those models actually occurs.